Supplementary file for
Global ocean and sea ice variability simulated in eddy-permitting climate models

Yushi Morioka[1], Eric Maisonnave[2], Sébastien Masson[2], Clement Rousset[2],
Luis Kornblueh[3], Marco Giorgetta[3], Masami Nonaka[1], Swadhin K. Behera[1]

1: Application Laboratory, VAiG, JAMSTEC, Yokohama, Japan
2: LOCEAN-IPSL, Sorbonne Université, Paris, France
3: Max Planck Institute for Meteorology, Hamburg, Germany

May 14, 2025 (submitted)
Geoscientific Model Development

Corresponding Author: Yushi Morioka
Showamachi 3173-25, Kanazawa-ku, Yokohama, JAPAN
morioka@jamstec.go.jp, +81-45-778-5509

Supplementary Figures

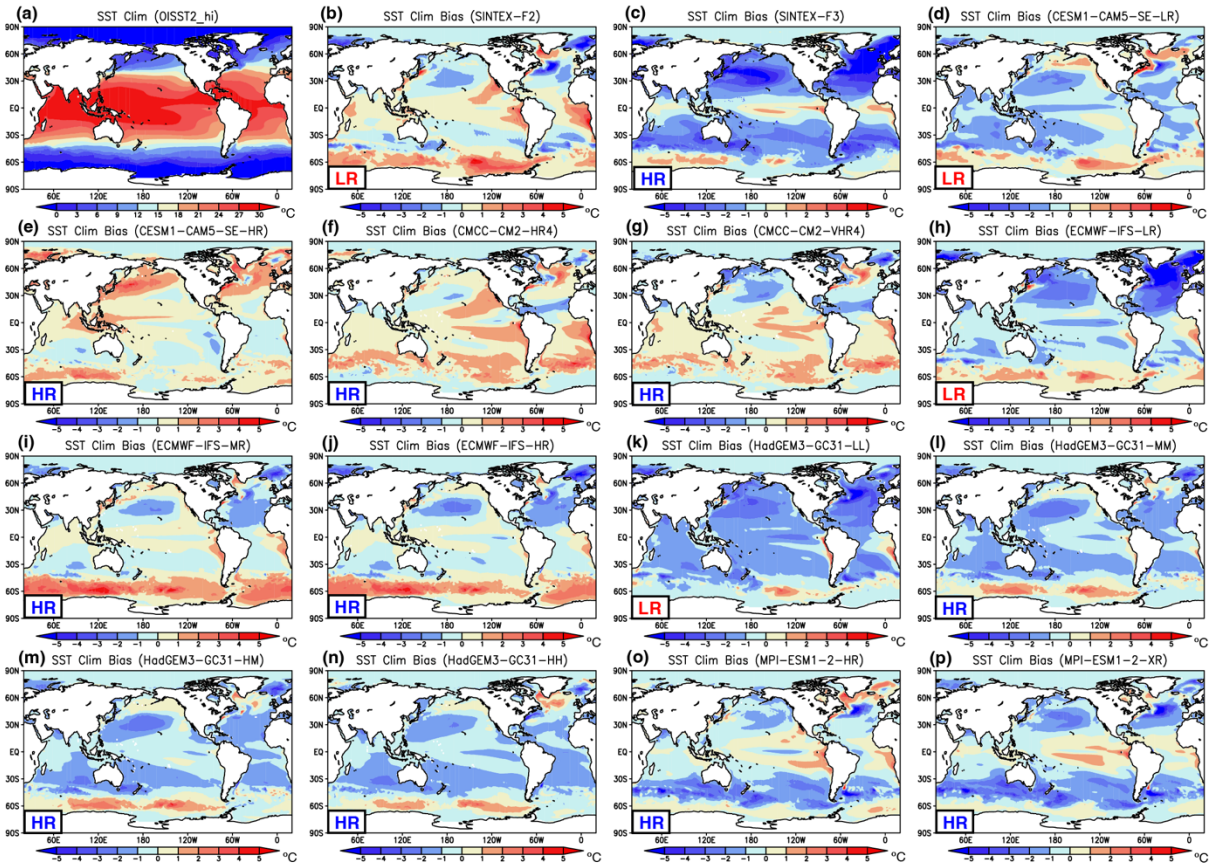

Supplementary Figure 1 (a) Annual mean of the observed sea surface temperature (SST, in ºC) during 1982-2022 from the OISST2_hi dataset. **(b)** Difference in the annual mean SST (in ºC) between the SINTEX-F2 model and the OISST2_hi (i.e., model minus observation). **(c-p)** Same as in (b), but for the SINTEX-F3, CESM1-CAM5-SE-LR, CESM1-CAM5-SE-HR, CMCC-CM2-HR4, CMCC-CM2-VHR4, ECMWF-IFS-LR, ECMWF-IFS-MR, ECMWF-IFS-HR, HadGEM3-GC31-LL, HadGEM3-GC31-MM, HadGEM3-GC31-HM, HadGEM3-GC31-HH, MPI-ESM1-2-HR, and MPI-ESM1-2-XR models, respectively. The LR in the bottom left of the panel stands for the low-resolution model, whereas the HR corresponds to the high-resolution model.

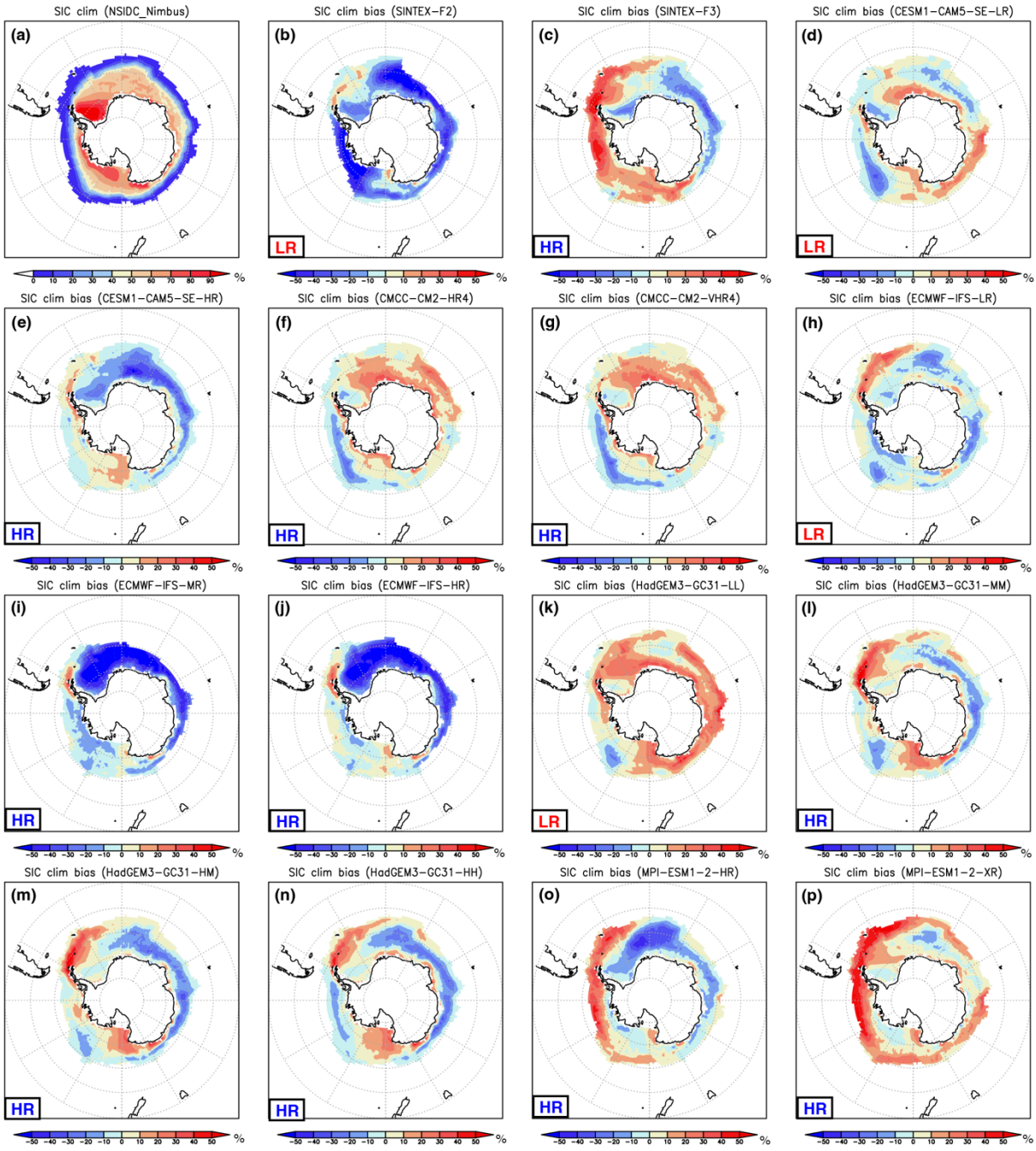

Supplementary Figure 2 (a) Annual mean of the observed sea ice concentration (SIC, in %) in the Antarctic Sea during 1982-2022 from the NSIDC_Nimbus dataset. **(b)** Difference in the annual mean SIC (in %) between the SINTEX-F2 model and the NSIDC_Nimbus data (i.e., model minus observation). **(c-p)** Same as in (b), but for the SINTEX-F3, CESM1-CAM5-SE-LR, CESM1-CAM5-SE-HR, CMCC-CM2-HR4, CMCC-CM2-VHR4, ECMWF-IFS-LR, ECMWF-IFS-MR, ECMWF-IFS-HR, HadGEM3-GC31-LL, HadGEM3-GC31-MM, HadGEM3-GC31-HM, HadGEM3-GC31-HH, MPI-ESM1-2-HR, and MPI-ESM1-2-XR models, respectively. The LR in the bottom left of the panel stands for the low-resolution model, whereas the HR corresponds to the high-resolution model.

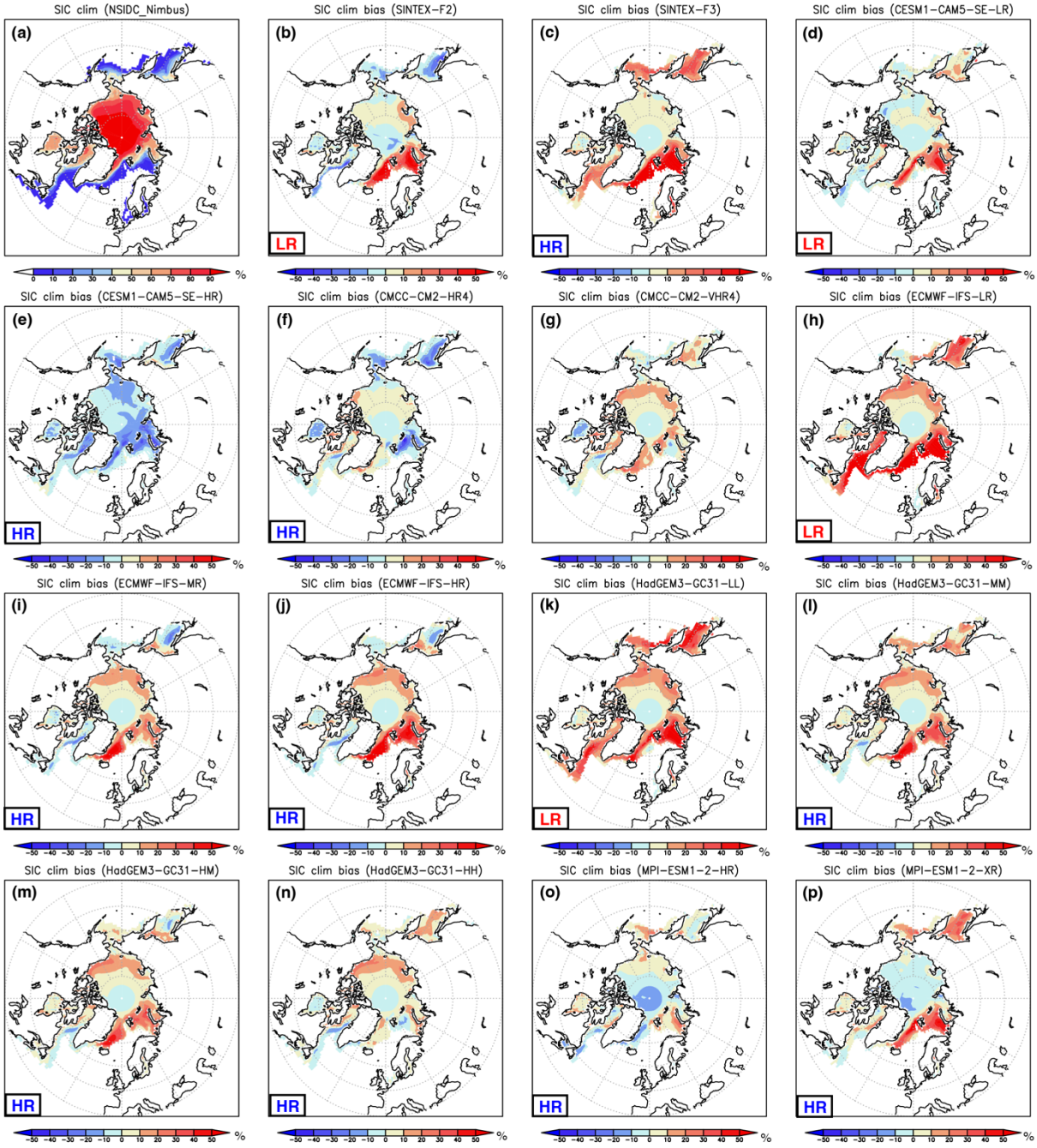

Supplementary Figure 3 Same as in Fig. S2, but for the Arctic Sea.

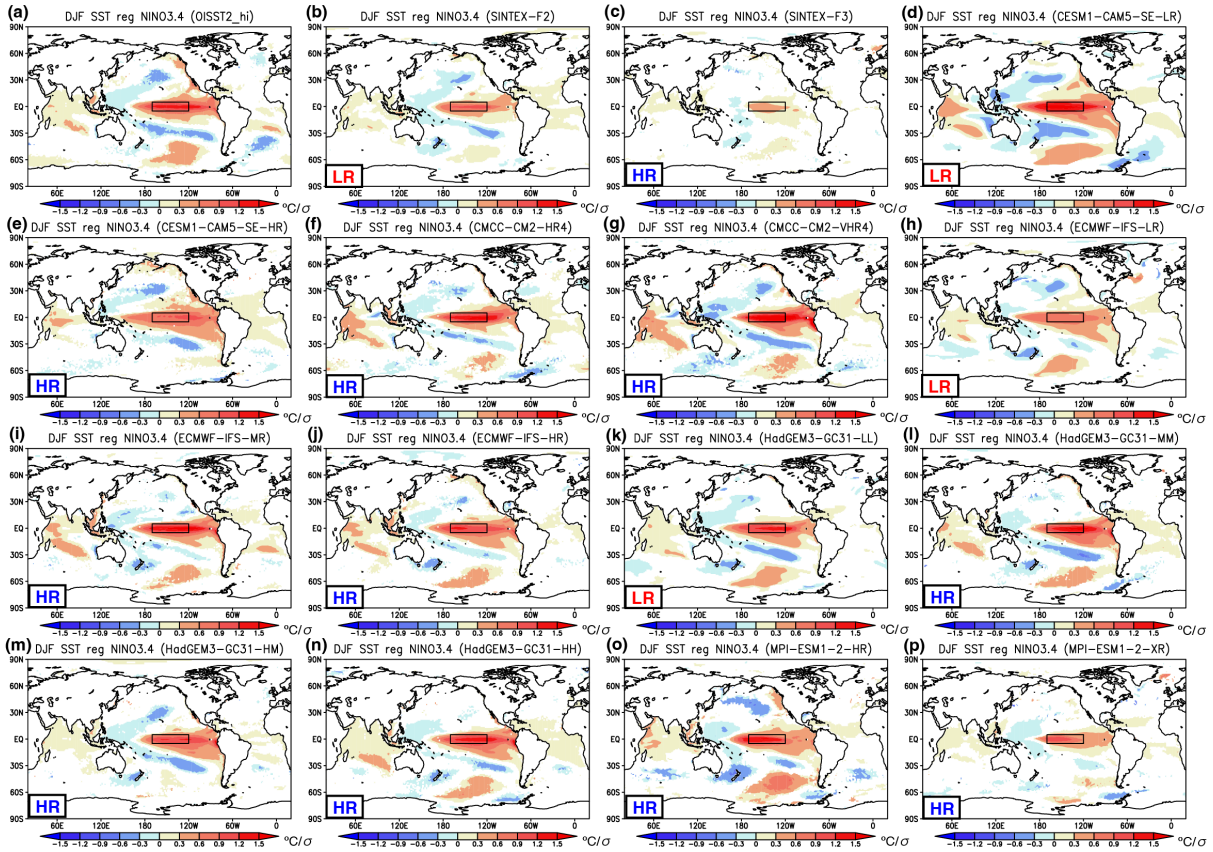

Supplementary Figure 4 (a) Spatial pattern of December-February mean SST anomalies (in ºC/ σ) regressed onto the standardized NINO3.4 index for the OISST2_hi data. Color indicates a statistically significant value that exceeds 90 % confidence level using a Student's *t*-test. A black box indicates a region in which we calculated the NINO3.4 index. **(b-p)** Same as in (a), but for the SINTEX-F2, SINTEX-F3, CESM1-CAM5-SE-LR, CESM1-CAM5-SE-HR, CMCC-CM2-HR4, CMCC-CM2-VHR4, ECMWF-IFS-LR, ECMWF-IFS-MR, ECMWF-IFS-HR, HadGEM3-GC31-LL, HadGEM3-GC31-MM, HadGEM3-GC31-HM, HadGEM3-GC31-HH, MPI-ESM1-2-HR, and MPI-ESM1-2-XR models, respectively. The LR in the bottom left of the panel stands for the low-resolution model, whereas the HR corresponds to the high-resolution model.

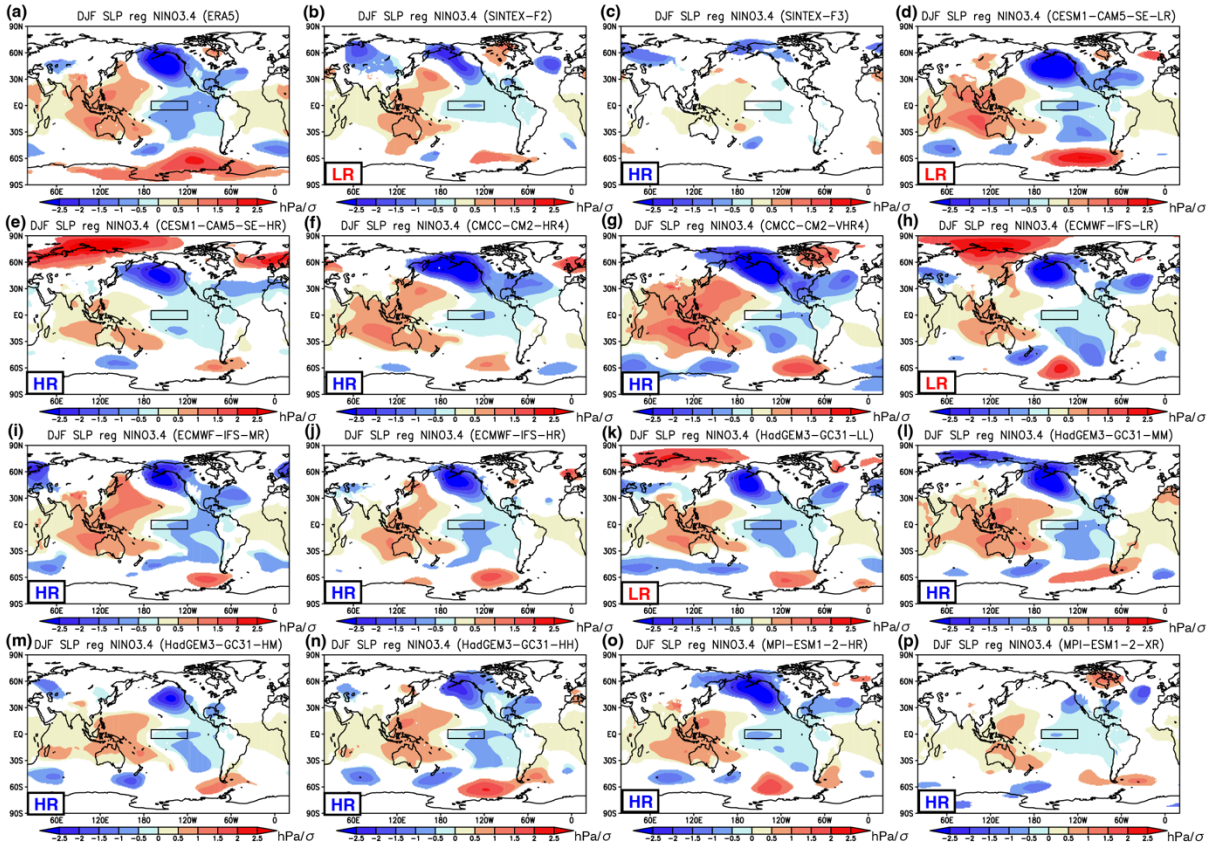

Supplementary Figure 5 (a) Spatial pattern of December-February mean SLP anomalies (in hPa/ σ) regressed onto the standardized NINO3.4 index for the ERA5 reanalysis product. Color indicates a statistically significant value that exceeds 90 % confidence level using a Student's *t*-test. A black box indicates a region in which we calculated the NINO3.4 index. **(b-p)** Same as in (a), but for the SINTEX-F2, SINTEX-F3, CESM1-CAM5-SE-LR, CESM1-CAM5-SE-HR, CMCC-CM2-HR4, CMCC-CM2-VHR4, ECMWF-IFS-LR, ECMWF-IFS-MR, ECMWF-IFS-HR, HadGEM3-GC31-LL, HadGEM3-GC31-MM, HadGEM3-GC31-HM, HadGEM3-GC31-HH, MPI-ESM1-2-HR, and MPI-ESM1-2-XR models, respectively. The LR in the bottom left of the panel stands for the low-resolution model, whereas the HR corresponds to the high-resolution model.

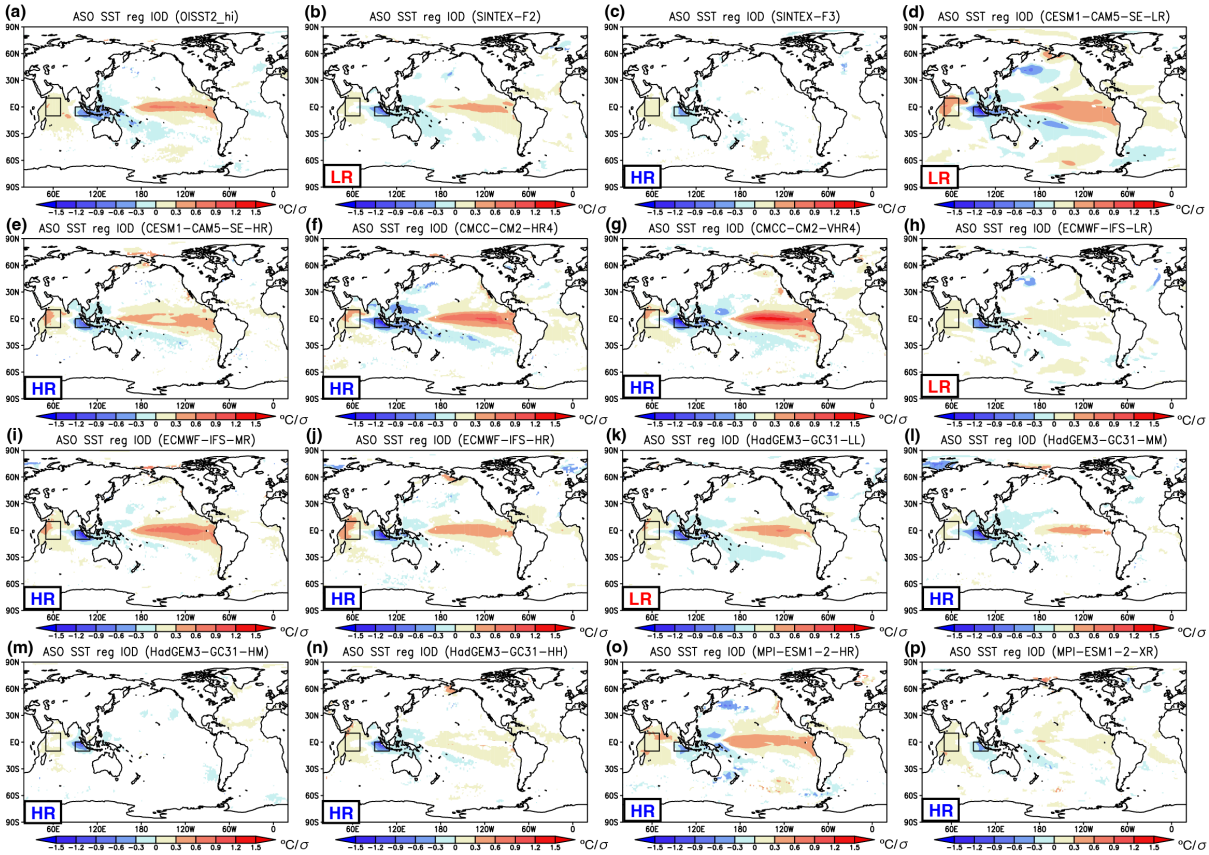

Supplementary Figure 6 Same as in Fig. S4, for the August-October mean SST anomalies (in ºC/ σ) regressed onto the standardized Dipole Mode index of the Indian Ocean Dipole.

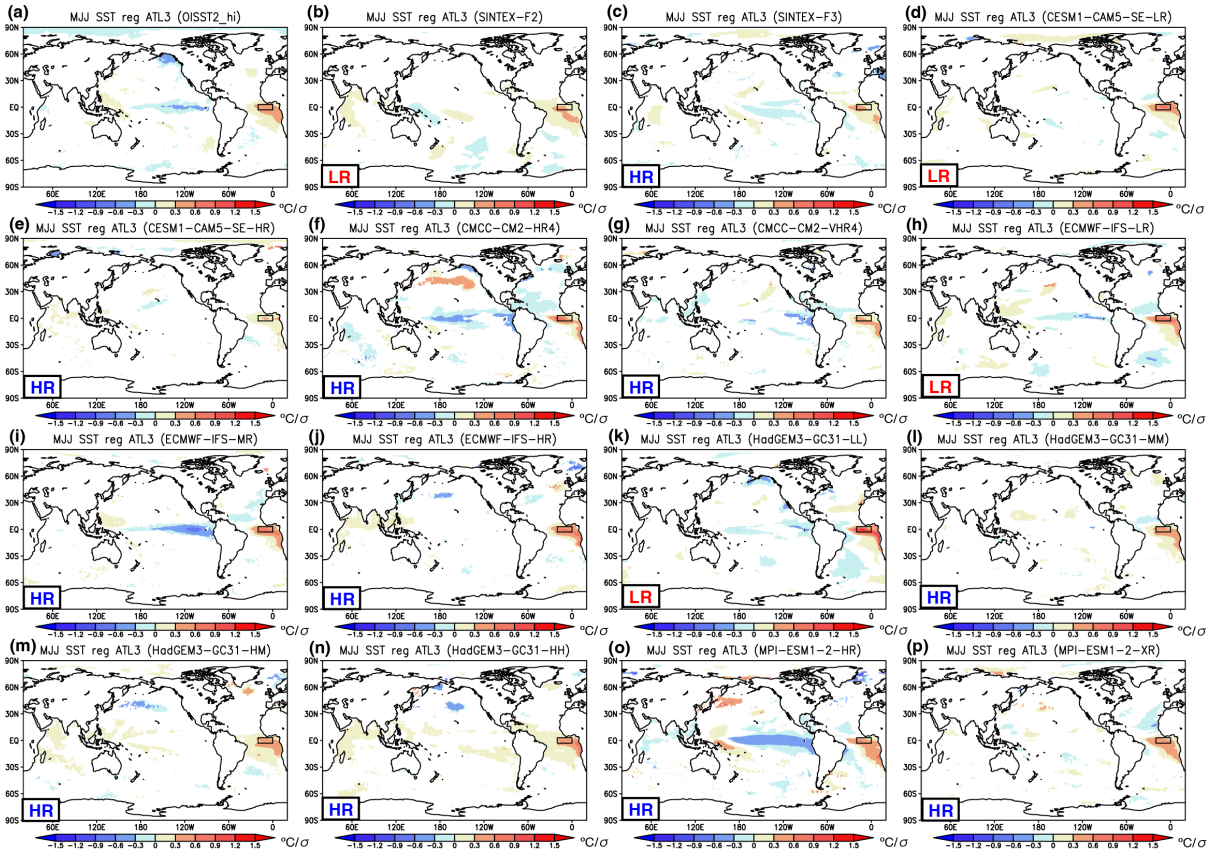

Supplementary Figure 7 Same as in Fig. S6, for the May-July mean SST anomalies (in ºC/ σ) regressed onto the standardized ATL3 index of the Atlantic Niño/Niña.

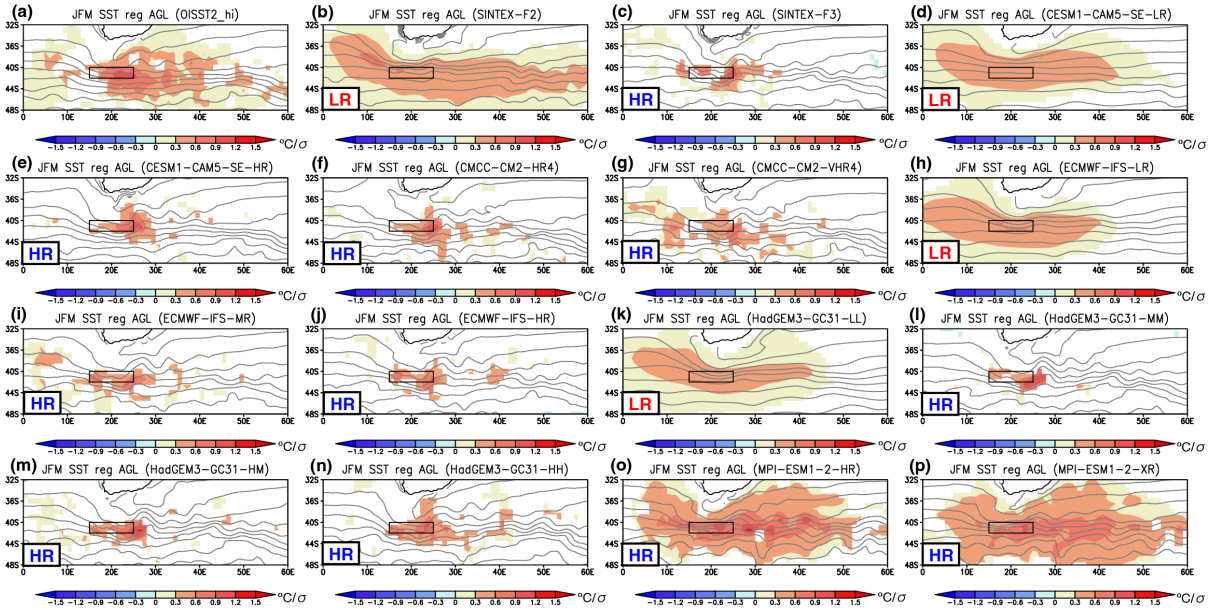

Supplementary Figure 8 (a) Spatial pattern of January-March mean SST climatology (gray contour, C.I. 2 ºC) and SST anomalies (in ºC/ σ) regressed onto the standardized SST index over the Agulhas Retroflection Current (15ºE-30ºE, 42ºS-40ºS; black box) region for the OISST2_hi data. Color indicates a statistically significant value that exceeds 90 % confidence level using a Student's *t*-test. **(b-p)** Same as in (a), but for the SINTEX-F2, SINTEX-F3, CESM1-CAM5-SE-LR, CESM1-CAM5-SE-HR, CMCC-CM2-HR4, CMCC-CM2-VHR4, ECMWF-IFS-LR, ECMWF-IFS-MR, ECMWF-IFS-HR, HadGEM3-GC31-LL, HadGEM3-GC31-MM, HadGEM3-GC31-HM, HadGEM3-GC31-HH, MPI-ESM1-2-HR, and MPI-ESM1-2-XR models, respectively. The LR in the bottom left of the panel stands for the low-resolution model, whereas the HR corresponds to the high-resolution model.

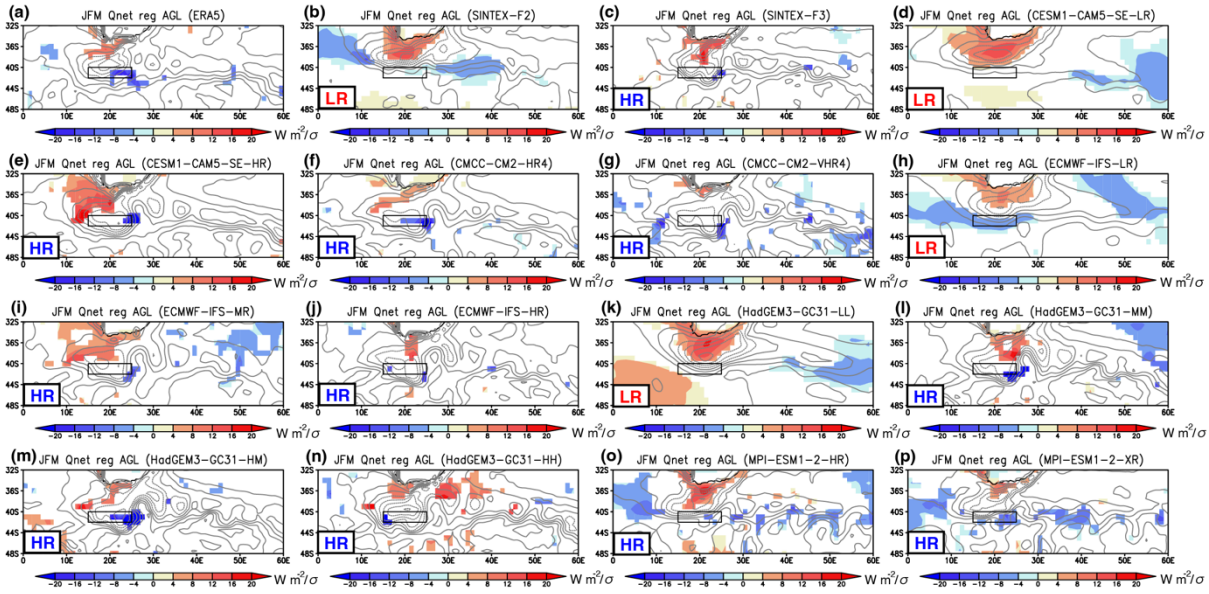

Supplementary Figure 9 (a) Spatial pattern of January-March mean net surface heat flux climatology (gray contour, C.I. 30 W m^{-2}/ σ) and net surface heat flux anomalies (in W m^{-2}/ σ) regressed onto the standardized SST index over the Agulhas Retroflection Current (15ºE-30ºE, 42ºS-40ºS; black box) region for the ERA5 reanalysis product. Color indicates a statistically significant value that exceeds 80 % confidence level using a Student's *t*-test. Positive values indicate the heat going into the ocean. **(b-p)** Same as in (a), but for the SINTEX-F2, SINTEX-F3, CESM1-CAM5-SE-LR, CESM1-CAM5-SE-HR, CMCC-CM2-HR4, CMCC-CM2-VHR4, ECMWF-IFS-LR, ECMWF-IFS-MR, ECMWF-IFS-HR, HadGEM3-GC31-LL, HadGEM3-GC31-MM, HadGEM3-GC31-HM, HadGEM3-GC31-HH, MPI-ESM1-2-HR, and MPI-ESM1-2-XR models, respectively. The LR in the bottom left of the panel stands for the low-resolution model, whereas the HR corresponds to the high-resolution model.

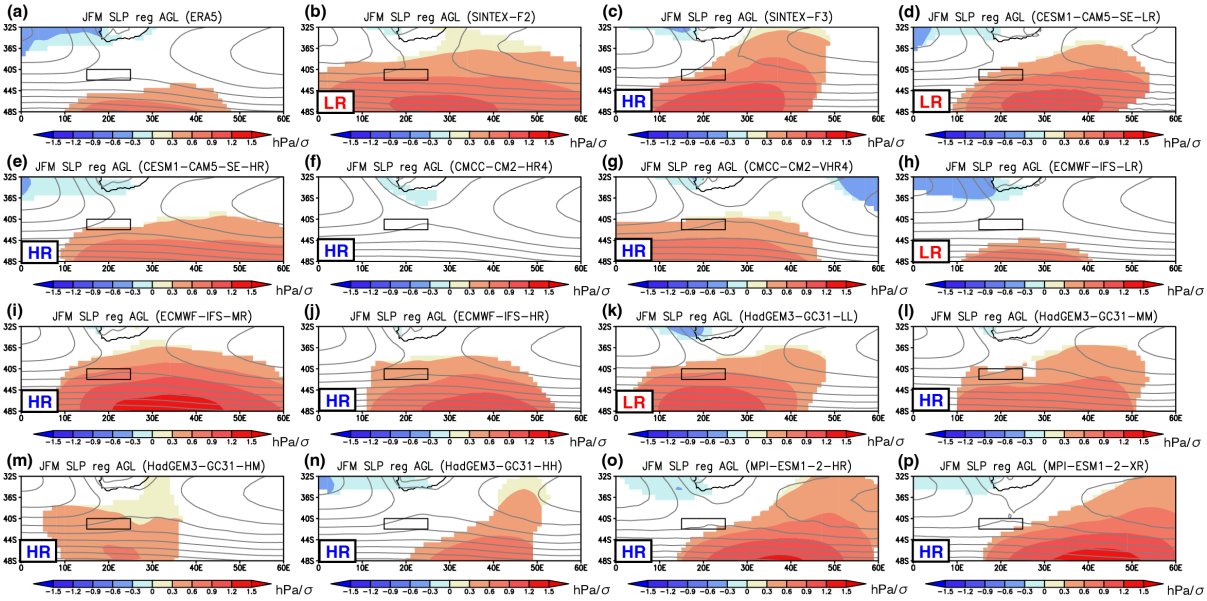

Supplementary Figure 10 (a) Spatial pattern of January-March mean SLP climatology (gray contour, C.I. 2 hPa) and SLP anomalies (in hPa/ σ) regressed onto the standardized SST index over the Agulhas Retroflection Current (15ºE-30ºE, 42ºS-40ºS; black box) region for the ERA5 reanalysis product. Color indicates a statistically significant value that exceeds 90 % confidence level using a Student's *t*-test. **(b-p)** Same as in (a), but for the SINTEX-F2, SINTEX-F3, CESM1-CAM5-SE-LR, CESM1-CAM5-SE-HR, CMCC-CM2-HR4, CMCC-CM2-VHR4, ECMWF-IFS-LR, ECMWF-IFS-MR, ECMWF-IFS-HR, HadGEM3-GC31-LL, HadGEM3-GC31-MM, HadGEM3-GC31-HM, HadGEM3-GC31-HH, MPI-ESM1-2-HR, and MPI-ESM1-2-XR models, respectively. The LR in the bottom left of the panel stands for the low-resolution model, whereas the HR corresponds to the high-resolution model.

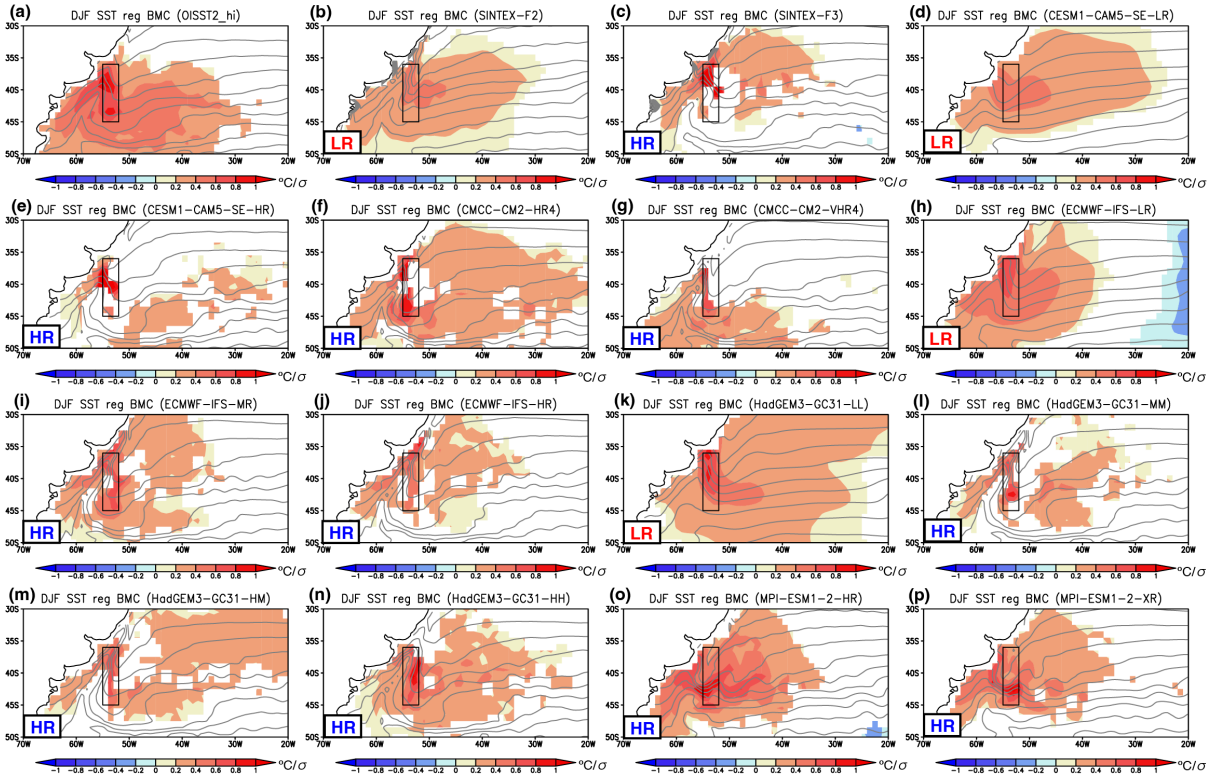

Supplementary Figure 11 (a) Spatial pattern of December-February mean SST climatology (gray contour, C.I. 2 ºC) and SST anomalies (in ºC/ σ) regressed onto the standardized SST index over the Brazil-Malvinas Current (55ºW-52ºW, 45ºS-36ºS) region for the OISST2_hi data. Color indicates a statistically significant value that exceeds 90 % confidence level using a Student's *t*-test. **(b-p)** Same as in (a), but for the SINTEX-F2, SINTEX-F3, CESM1-CAM5-SE-LR, CESM1-CAM5-SE-HR, CMCC-CM2-HR4, CMCC-CM2-VHR4, ECMWF-IFS-LR, ECMWF-IFS-MR, ECMWF-IFS-HR, HadGEM3-GC31-LL, HadGEM3-GC31-MM, HadGEM3-GC31-HM, HadGEM3-GC31-HH, MPI-ESM1-2-HR, and MPI-ESM1-2-XR models, respectively. The LR in the bottom left of the panel stands for the low-resolution model, whereas the HR corresponds to the high-resolution model.

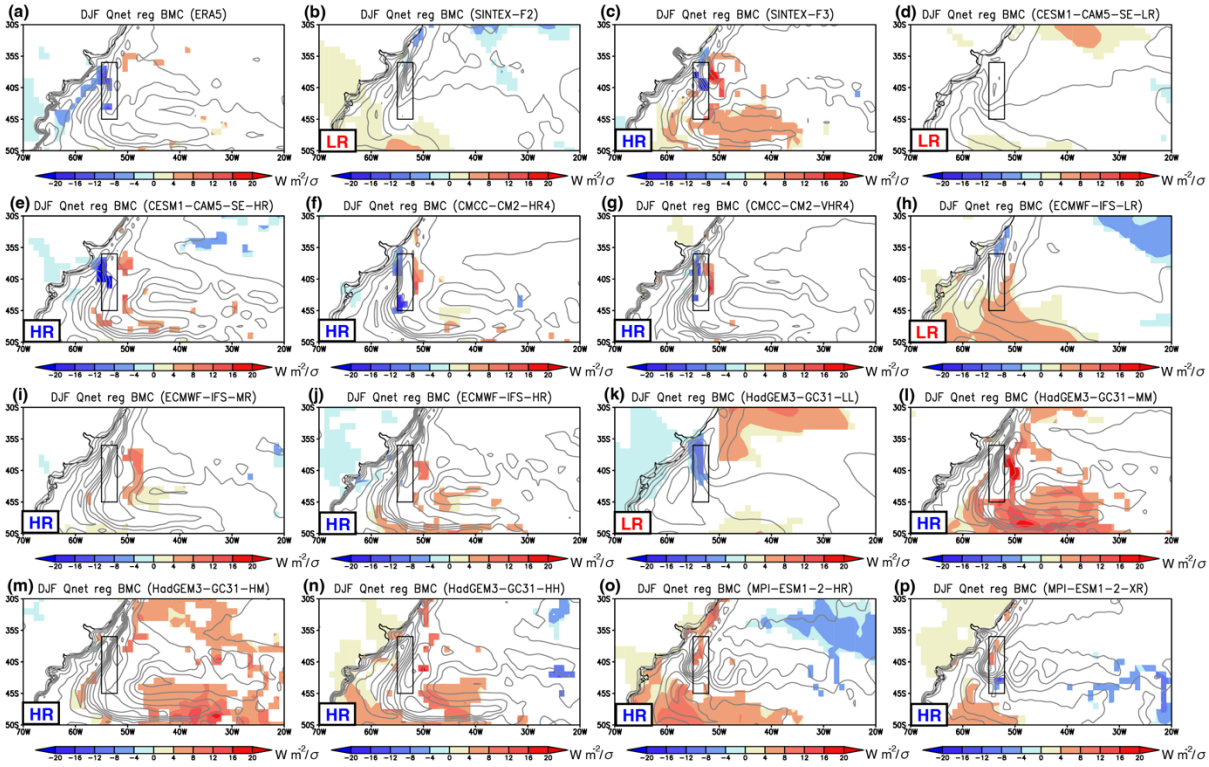

Supplementary Figure 12 (a) Spatial pattern of December-February mean net surface heat flux climatology (gray contour, C.I. 30 W m^{-2}/σ) and net surface heat flux anomalies (in W m^{-2}/σ) regressed onto the standardized SST index over the Brazil-Malvinas Current (55ºW-52ºW, 45ºS-36ºS) region for the ERA5 reanalysis product. Color indicates a statistically significant value that exceeds 80 % confidence level using a Student's *t*-test. Positive values indicate the heat going into the ocean. **(b-p)** Same as in (a), but for the SINTEX-F2, SINTEX-F3, CESM1-CAM5-SE-LR, CESM1-CAM5-SE-HR, CMCC-CM2-HR4, CMCC-CM2-VHR4, ECMWF-IFS-LR, ECMWF-IFS-MR, ECMWF-IFS-HR, HadGEM3-GC31-LL, HadGEM3-GC31-MM, HadGEM3-GC31-HM, HadGEM3-GC31-HH, MPI-ESM1-2-HR, and MPI-ESM1-2-XR models, respectively. The LR in the bottom left of the panel stands for the low-resolution model, whereas the HR corresponds to the high-resolution model.

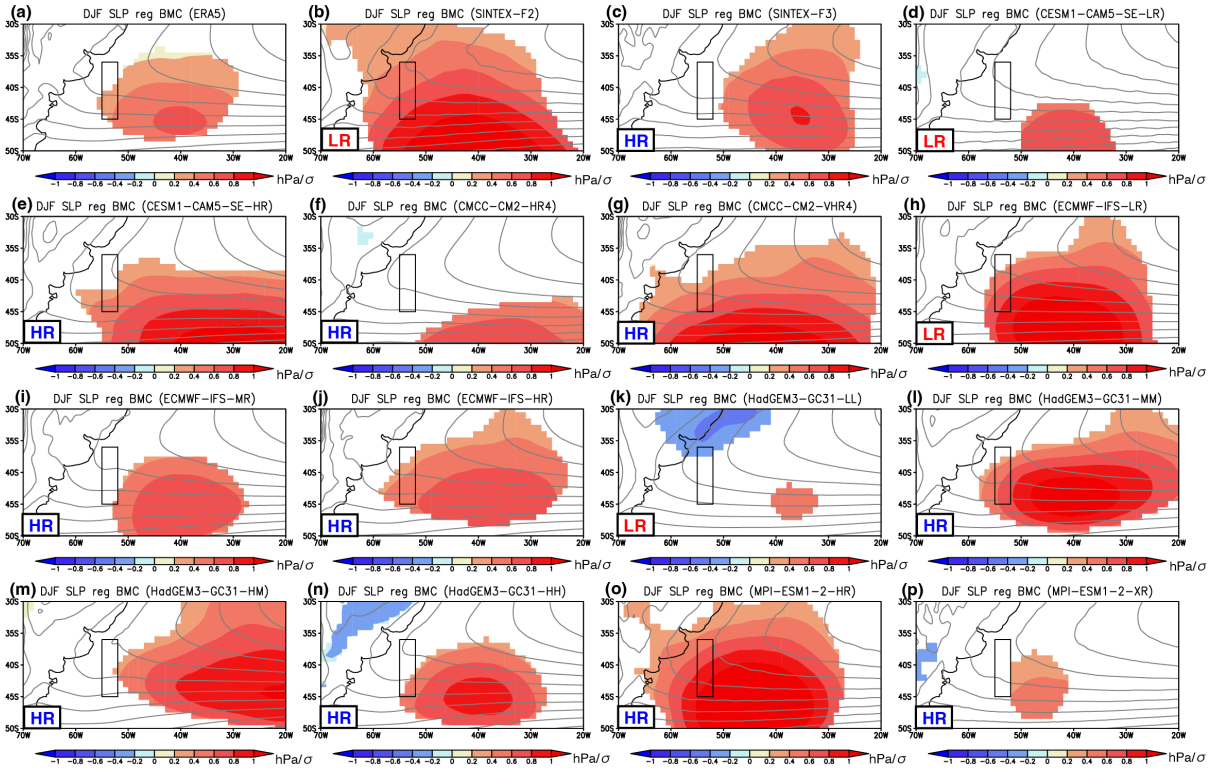

Supplementary Figure 13 (a) Spatial pattern of December-February mean SLP climatology (gray contour, C.I. 2 hPa) and SLP anomalies (in hPa/ σ) regressed onto the standardized SST index over the Brazil-Malvinas Current (55ºW-52ºW, 45ºS-36ºS) region for the ERA5 reanalysis product. Color indicates a statistically significant value that exceeds 90 % confidence level using a Student's *t*-test. **(b-p)** Same as in (a), but for the SINTEX-F2, SINTEX-F3, CESM1-CAM5-SE-LR, CESM1-CAM5-SE-HR, CMCC-CM2-HR4, CMCC-CM2-VHR4, ECMWF-IFS-LR, ECMWF-IFS-MR, ECMWF-IFS-HR, HadGEM3-GC31-LL, HadGEM3-GC31-MM, HadGEM3-GC31-HM, HadGEM3-GC31-HH, MPI-ESM1-2-HR, and MPI-ESM1-2-XR models, respectively. The LR in the bottom left of the panel stands for the low-resolution model, whereas the HR corresponds to the high-resolution model.

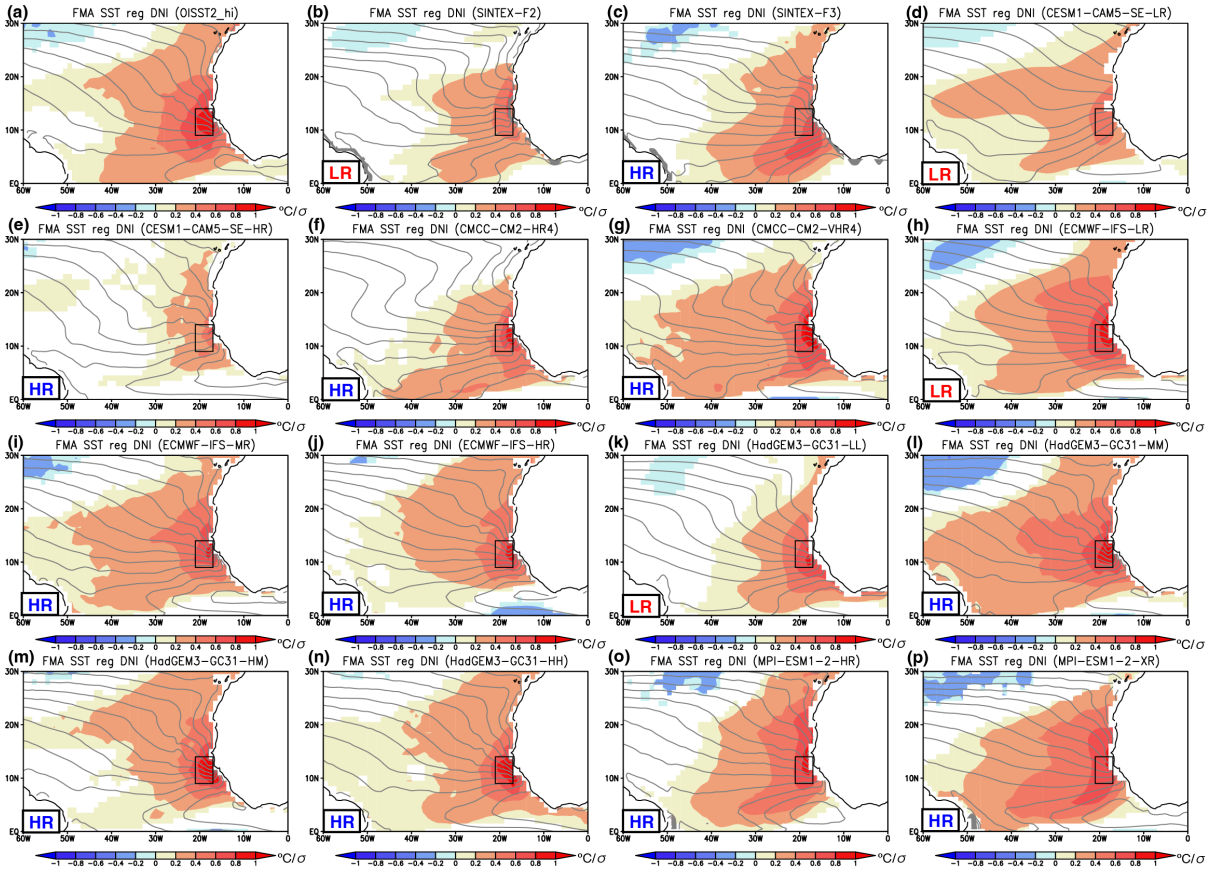

159

160 **Supplementary Figure 14 (a)** Spatial pattern of February-April mean SST climatology (gray
161 contour, C.I. 1 ºC) and SST anomalies (in ºC/ σ) regressed onto the standardized Dakar
162 Niño/Niña SST index (DNI; 21ºW-17ºW, 9ºN-14ºN in a black box) for the OISST2_hi dataset.
163 Color indicates a statistically significant value that exceeds 90 % confidence level using a
164 Student's *t*-test. **(b-p)** Same as in (a), but for the SINTEX-F2, SINTEX-F3, CESM1-CAM5-
165 SE-LR, CESM1-CAM5-SE-HR, CMCC-CM2-HR4, CMCC-CM2-VHR4, ECMWF-IFS-LR,
166 ECMWF-IFS-MR, ECMWF-IFS-HR, HadGEM3-GC31-LL, HadGEM3-GC31-MM,
167 HadGEM3-GC31-HM, HadGEM3-GC31-HH, MPI-ESM1-2-HR, and MPI-ESM1-2-XR
168 models, respectively. The LR in the bottom left of the panel stands for the low-resolution model,
169 whereas the HR corresponds to the high-resolution model.

170

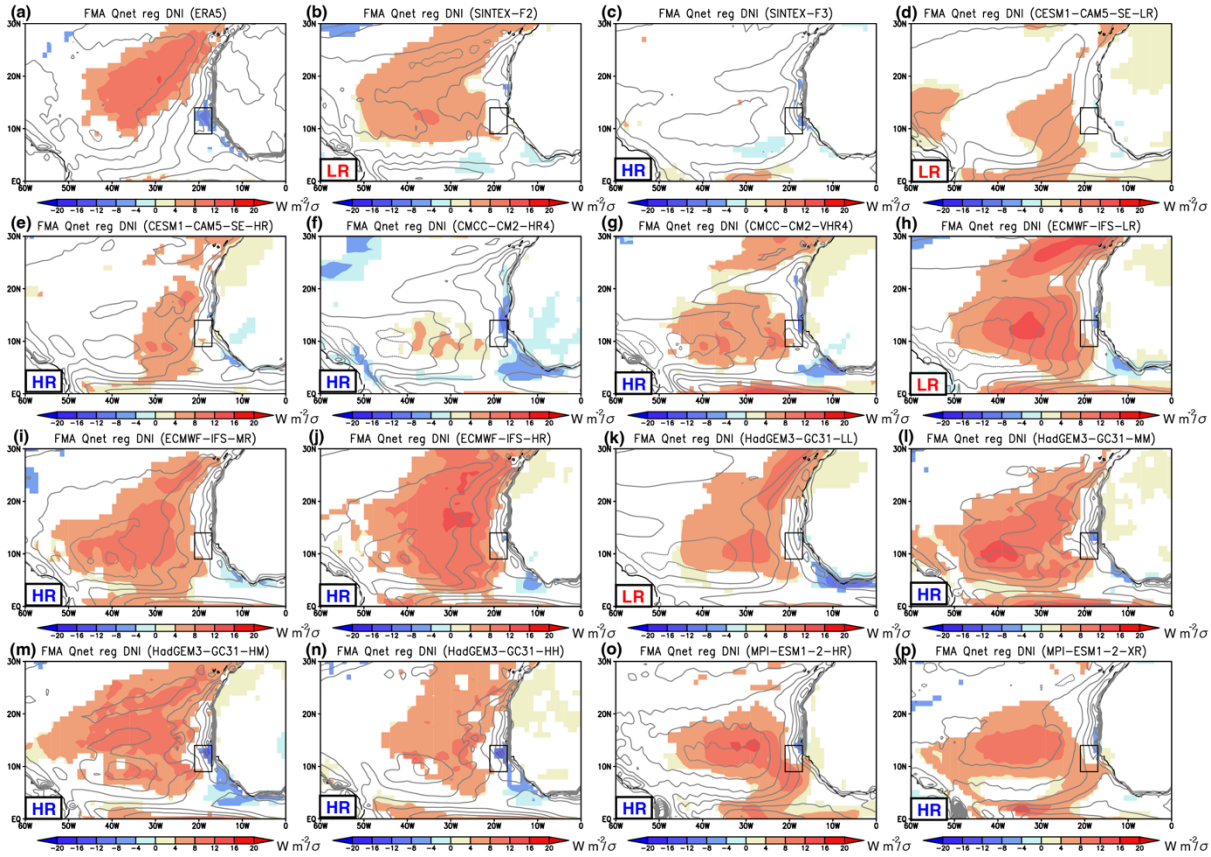

Supplementary Figure 15 (a) Spatial pattern of February-April mean net surface heat flux climatology (gray contour, C.I. 20 W m^{-2}/ σ) and net surface heat flux anomalies (in W m^{-2}/ σ) regressed onto the standardized Dakar Niño/Niña SST index (DNI; 21ºW-17ºW, 9ºN-14ºN in a black box) for the ERA5 reanalysis product. Color indicates a statistically significant value that exceeds 80 % confidence level using a Student's *t*-test. Positive values indicate the heat going into the ocean. **(b-p)** Same as in (a), but for the SINTEX-F2, SINTEX-F3, CESM1-CAM5-SE-LR, CESM1-CAM5-SE-HR, CMCC-CM2-HR4, CMCC-CM2-VHR4, ECMWF-IFS-LR, ECMWF-IFS-MR, ECMWF-IFS-HR, HadGEM3-GC31-LL, HadGEM3-GC31-MM, HadGEM3-GC31-HM, HadGEM3-GC31-HH, MPI-ESM1-2-HR, and MPI-ESM1-2-XR models, respectively. The LR in the bottom left of the panel stands for the low-resolution model, whereas the HR corresponds to the high-resolution model.

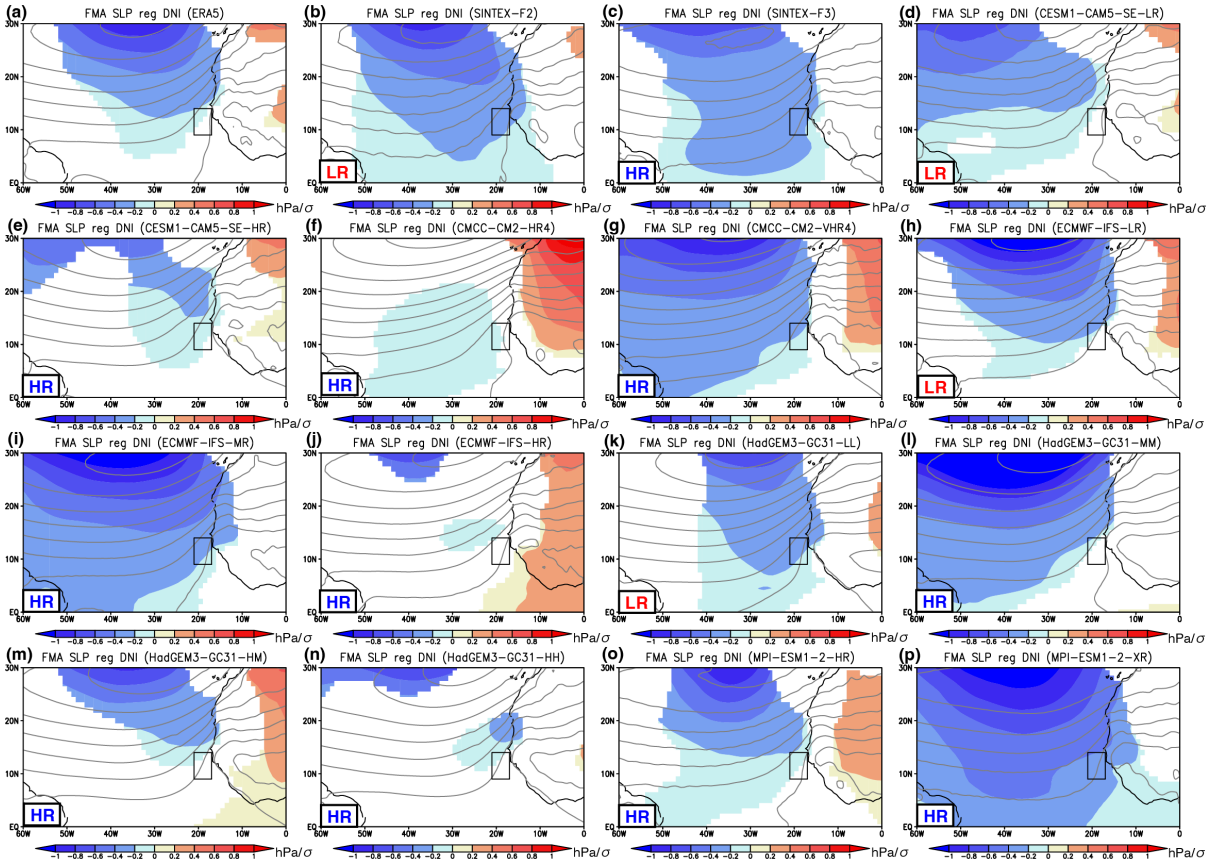

Supplementary Figure 16 (a) Spatial pattern of February-April mean SLP climatology (gray contour, C.I. 1.5 hPa) and SLP anomalies (in hPa/ σ) regressed onto the standardized Dakar Niño/Niña SST index (DNI; 21ºW-17ºW, 9ºN-14ºN in a black box) for the ERA5 reanalysis product. Color indicates a statistically significant value that exceeds 90 % confidence level using a Student's *t*-test. **(b-p)** Same as in (a), but for the SINTEX-F2, SINTEX-F3, CESM1-CAM5-SE-LR, CESM1-CAM5-SE-HR, CMCC-CM2-HR4, CMCC-CM2-VHR4, ECMWF-IFS-LR, ECMWF-IFS-MR, ECMWF-IFS-HR, HadGEM3-GC31-LL, HadGEM3-GC31-MM, HadGEM3-GC31-HM, HadGEM3-GC31-HH, MPI-ESM1-2-HR, and MPI-ESM1-2-XR models, respectively. The LR in the bottom left of the panel stands for the low-resolution model, whereas the HR corresponds to the high-resolution model.

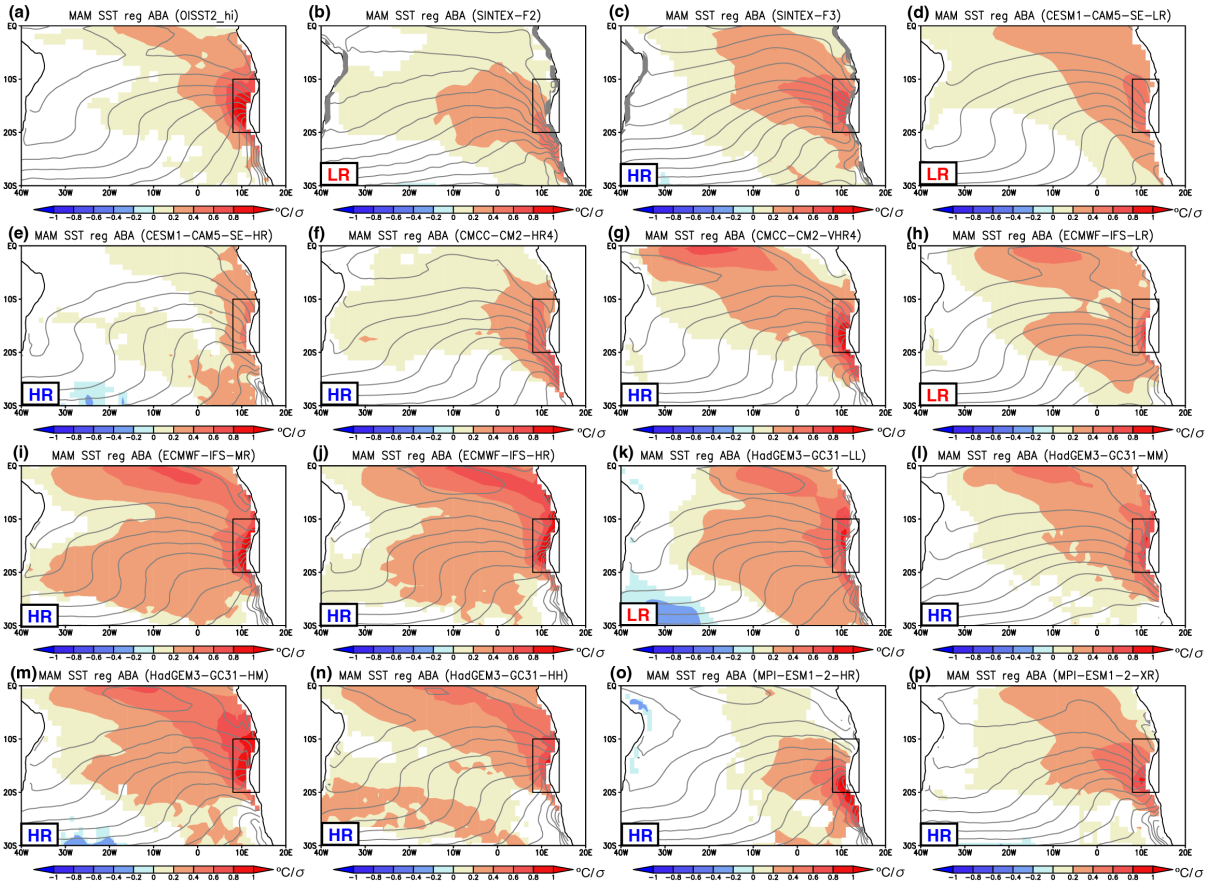

Supplementary Figure 17 (a) Spatial pattern of March-May mean SST climatology (gray contour, C.I. 1 ºC) and SST anomalies (in ºC/ σ) regressed onto the standardized Benguela Niño/Niña SST index (ABA; 8ºE-14ºE, 20ºS-10ºS in a black box) for the OISST2_hi dataset. Color indicates a statistically significant value that exceeds 90 % confidence level using a Student's *t*-test. **(b-p)** Same as in (a), but for the SINTEX-F2, SINTEX-F3, CESM1-CAM5-SE-LR, CESM1-CAM5-SE-HR, CMCC-CM2-HR4, CMCC-CM2-VHR4, ECMWF-IFS-LR, ECMWF-IFS-MR, ECMWF-IFS-HR, HadGEM3-GC31-LL, HadGEM3-GC31-MM, HadGEM3-GC31-HM, HadGEM3-GC31-HH, MPI-ESM1-2-HR, and MPI-ESM1-2-XR models, respectively. The LR in the bottom left of the panel stands for the low-resolution model, whereas the HR corresponds to the high-resolution model.

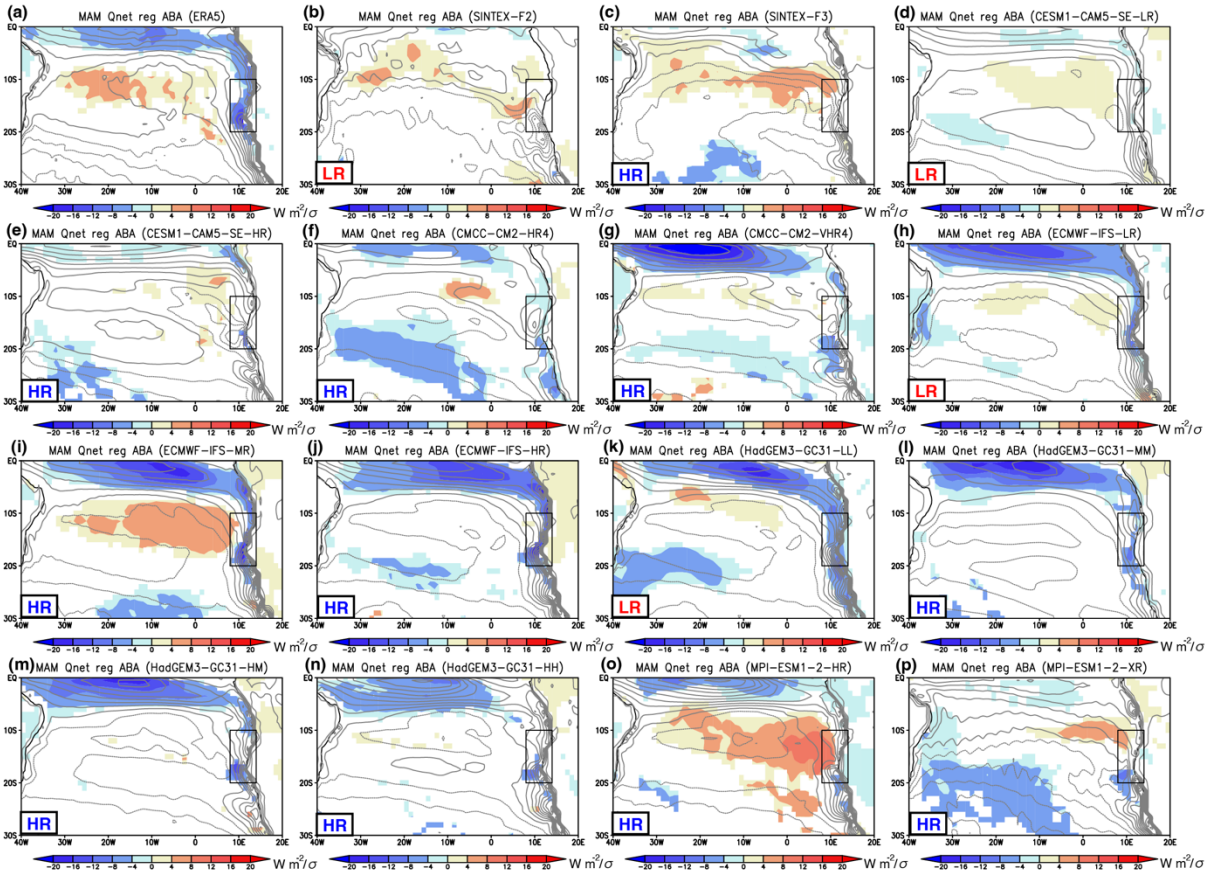

Supplementary Figure 18 (a) Spatial pattern of March-May mean net surface heat flux climatology (gray contour, C.I. 15 W m^{-2}/ σ) and net surface heat flux anomalies (in W m^{-2}/ σ) regressed onto the standardized Benguela Niño/Niña SST index (ABA; 8ºE-14ºE, 20ºS-10ºS in a black box) for the ERA5 reanalysis product. Color indicates a statistically significant value that exceeds 80 % confidence level using a Student's *t*-test. Positive values indicate the heat going into the ocean. **(b-p)** Same as in (a), but for the SINTEX-F2, SINTEX-F3, CESM1-CAM5-SE-LR, CESM1-CAM5-SE-HR, CMCC-CM2-HR4, CMCC-CM2-VHR4, ECMWF-IFS-LR, ECMWF-IFS-MR, ECMWF-IFS-HR, HadGEM3-GC31-LL, HadGEM3-GC31-MM, HadGEM3-GC31-HM, HadGEM3-GC31-HH, MPI-ESM1-2-HR, and MPI-ESM1-2-XR models, respectively. The LR in the bottom left of the panel stands for the low-resolution model, whereas the HR corresponds to the high-resolution model.

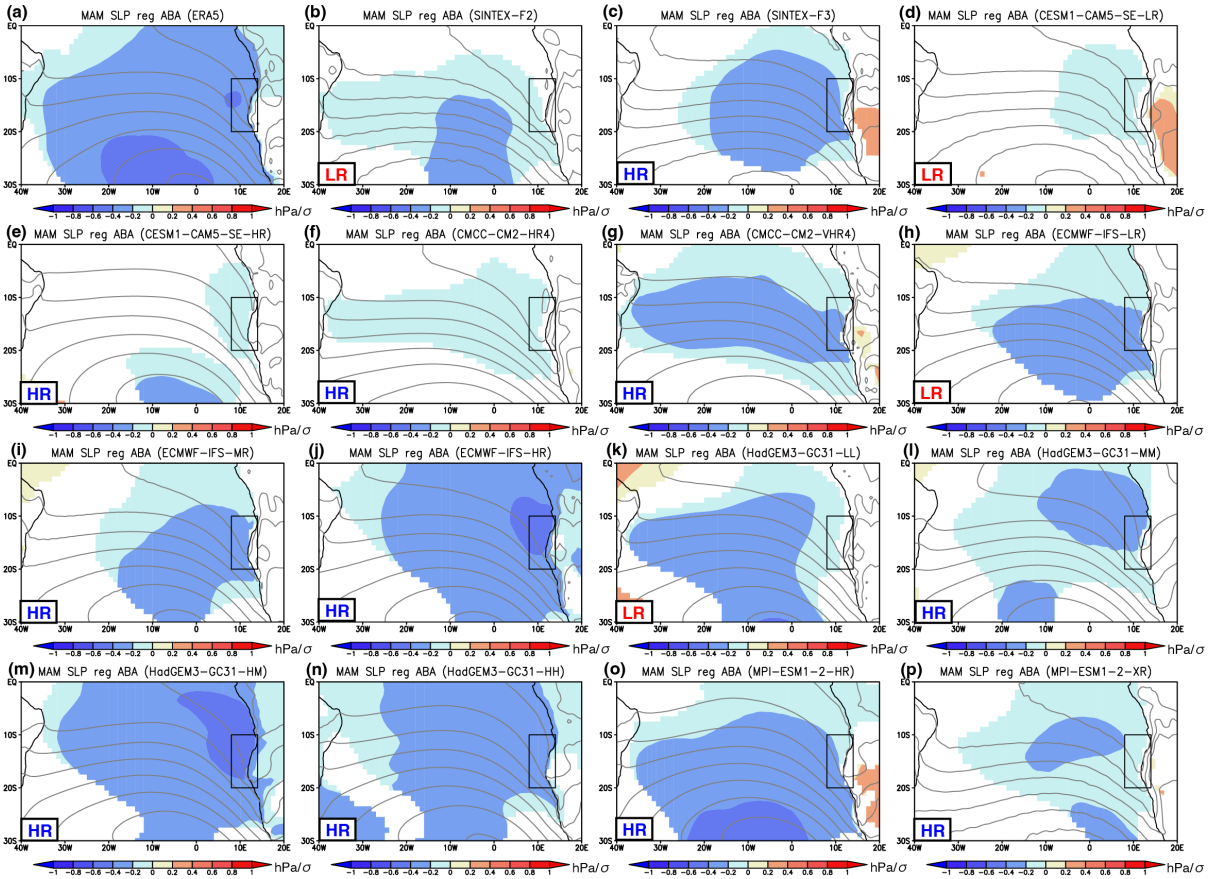

Supplementary Figure 19 (a) Spatial pattern of March-May mean SLP climatology (gray contour, C.I. 1.5 hPa) and SLP anomalies (in hPa/ σ) regressed onto the standardized Benguela Niño/Niña SST index (ABA; 8ºE-14ºE, 20ºS-10ºS in a black box) for the ERA5 reanalysis product. Color indicates a statistically significant value that exceeds 90 % confidence level using a Student's *t*-test. **(b-p)** Same as in (a), but for the SINTEX-F2, SINTEX-F3, CESM1-CAM5-SE-LR, CESM1-CAM5-SE-HR, CMCC-CM2-HR4, CMCC-CM2-VHR4, ECMWF-IFS-LR, ECMWF-IFS-MR, ECMWF-IFS-HR, HadGEM3-GC31-LL, HadGEM3-GC31-MM, HadGEM3-GC31-HM, HadGEM3-GC31-HH, MPI-ESM1-2-HR, and MPI-ESM1-2-XR models, respectively. The LR in the bottom left of the panel stands for the low-resolution model, whereas the HR corresponds to the high-resolution model.

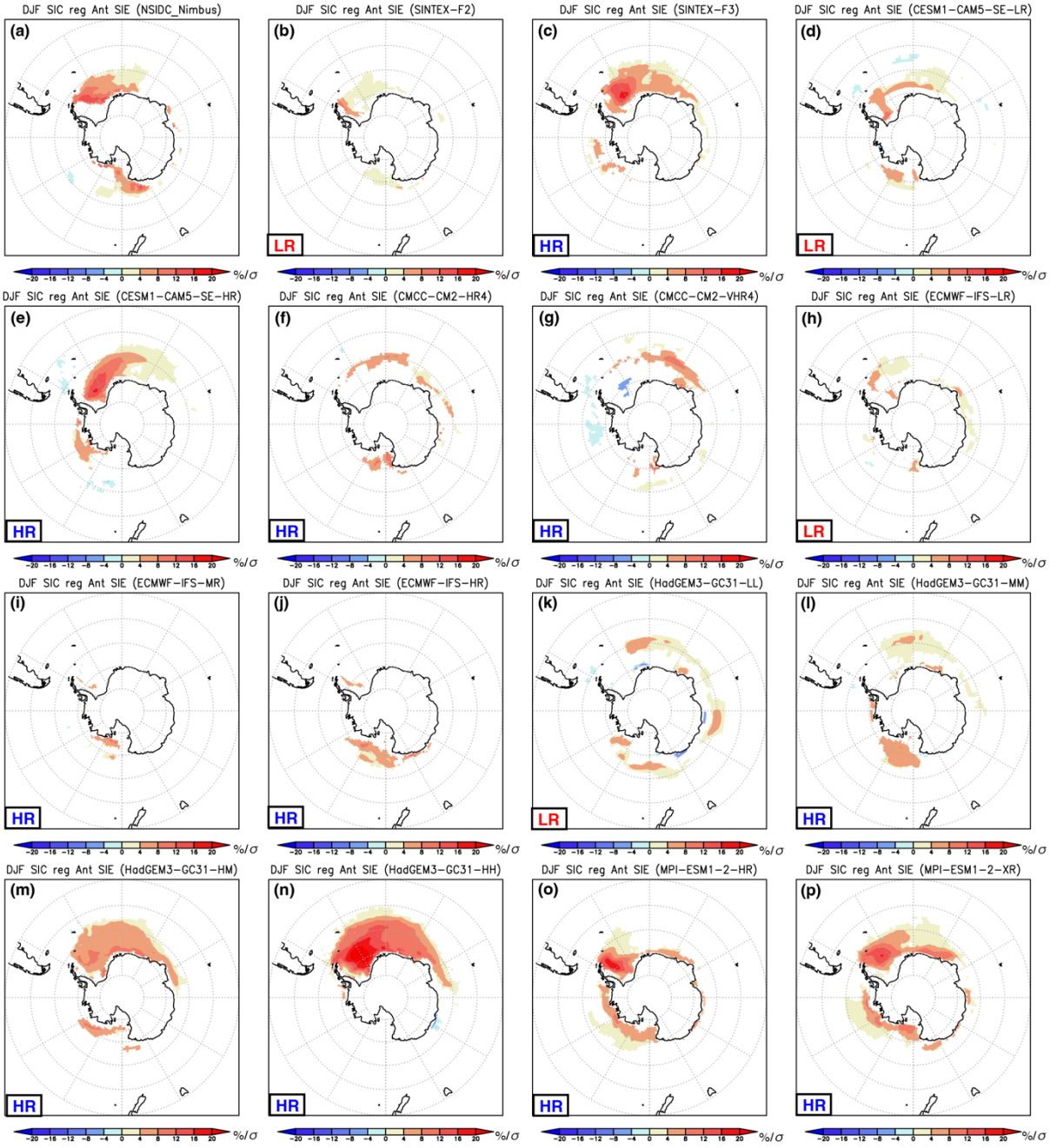

Supplementary Figure 20 (a) Spatial pattern of December-February mean sea ice concentration anomalies (SIC; in %/ σ) regressed onto the standardized Antarctic sea ice extent (SIE) anomalies for the NSIDC_Nimbus data. Color indicates a statistically significant value that exceeds 90 % confidence level using a Student's *t*-test. **(b-p)** Same as in (a), but for the SINTEX-F2, SINTEX-F3, CESM1-CAM5-SE-LR, CESM1-CAM5-SE-HR, CMCC-CM2-HR4, CMCC-CM2-VHR4, ECMWF-IFS-LR, ECMWF-IFS-MR, ECMWF-IFS-HR, HadGEM3-GC31-LL, HadGEM3-GC31-MM, HadGEM3-GC31-HM, HadGEM3-GC31-HH, MPI-ESM1-2-HR, and MPI-ESM1-2-XR models, respectively. The LR in the bottom left of

the panel stands for the low-resolution model, whereas the HR corresponds to the high-resolution model.

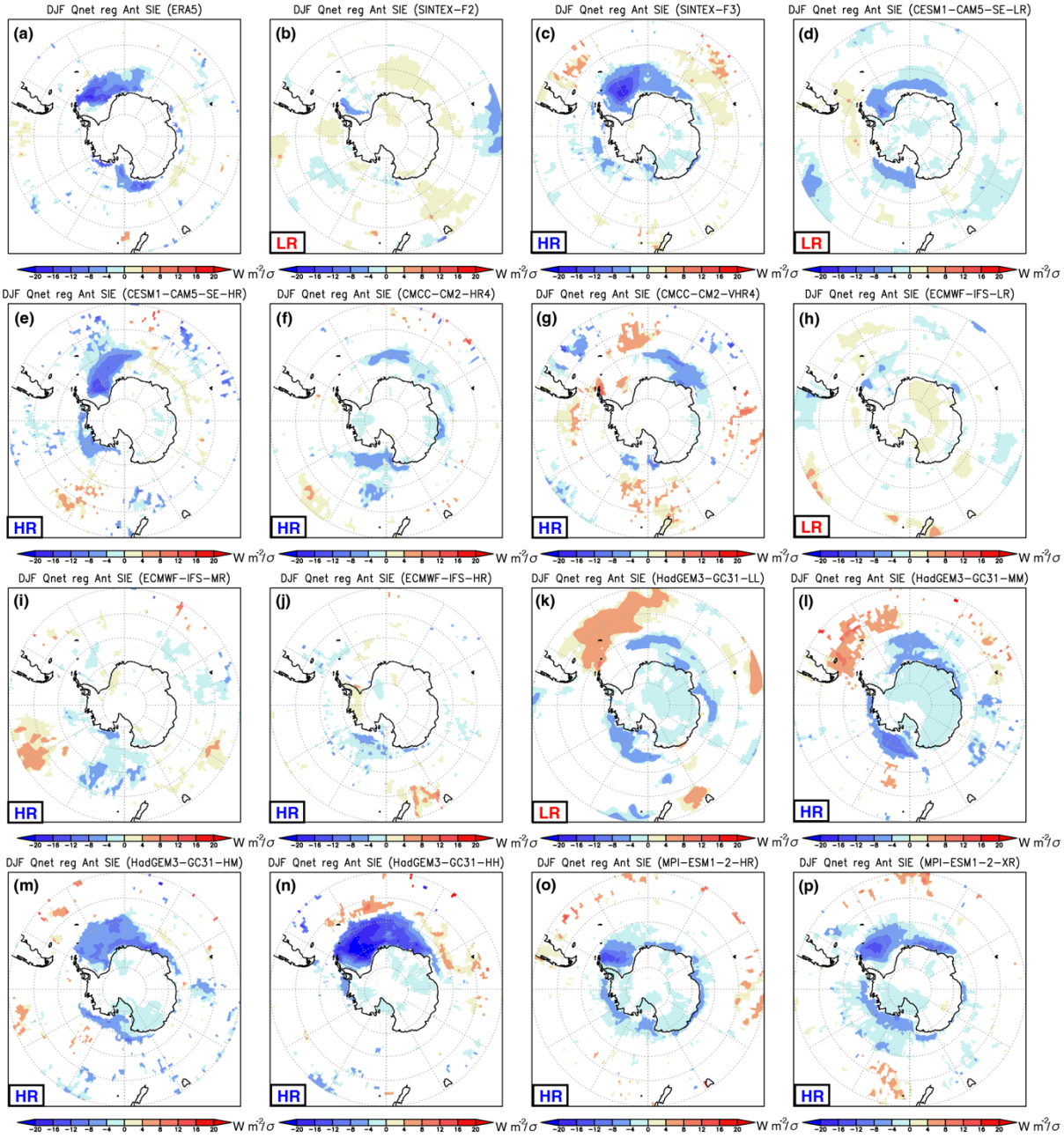

Supplementary Figure 21 (a) Spatial pattern of December-February mean net surface heat flux anomalies (in W m^{-2}/ σ) regressed onto the standardized Antarctic sea ice extent (SIE) anomalies for the NSIDC_Nimbus data. Color indicates a statistically significant value that exceeds 80 % confidence level using a Student's *t*-test. **(b-p)** Same as in (a), but for the SINTEX-F2, SINTEX-F3, CESM1-CAM5-SE-LR, CESM1-CAM5-SE-HR, CMCC-CM2-HR4, CMCC-CM2-VHR4, ECMWF-IFS-LR, ECMWF-IFS-MR, ECMWF-IFS-HR, HadGEM3-GC31-LL, HadGEM3-GC31-MM, HadGEM3-GC31-HM, HadGEM3-GC31-HH, MPI-ESM1-2-HR, and MPI-ESM1-2-XR models, respectively. The LR in the bottom left of the panel stands for the low-resolution model, whereas the HR corresponds to the high-resolution model.

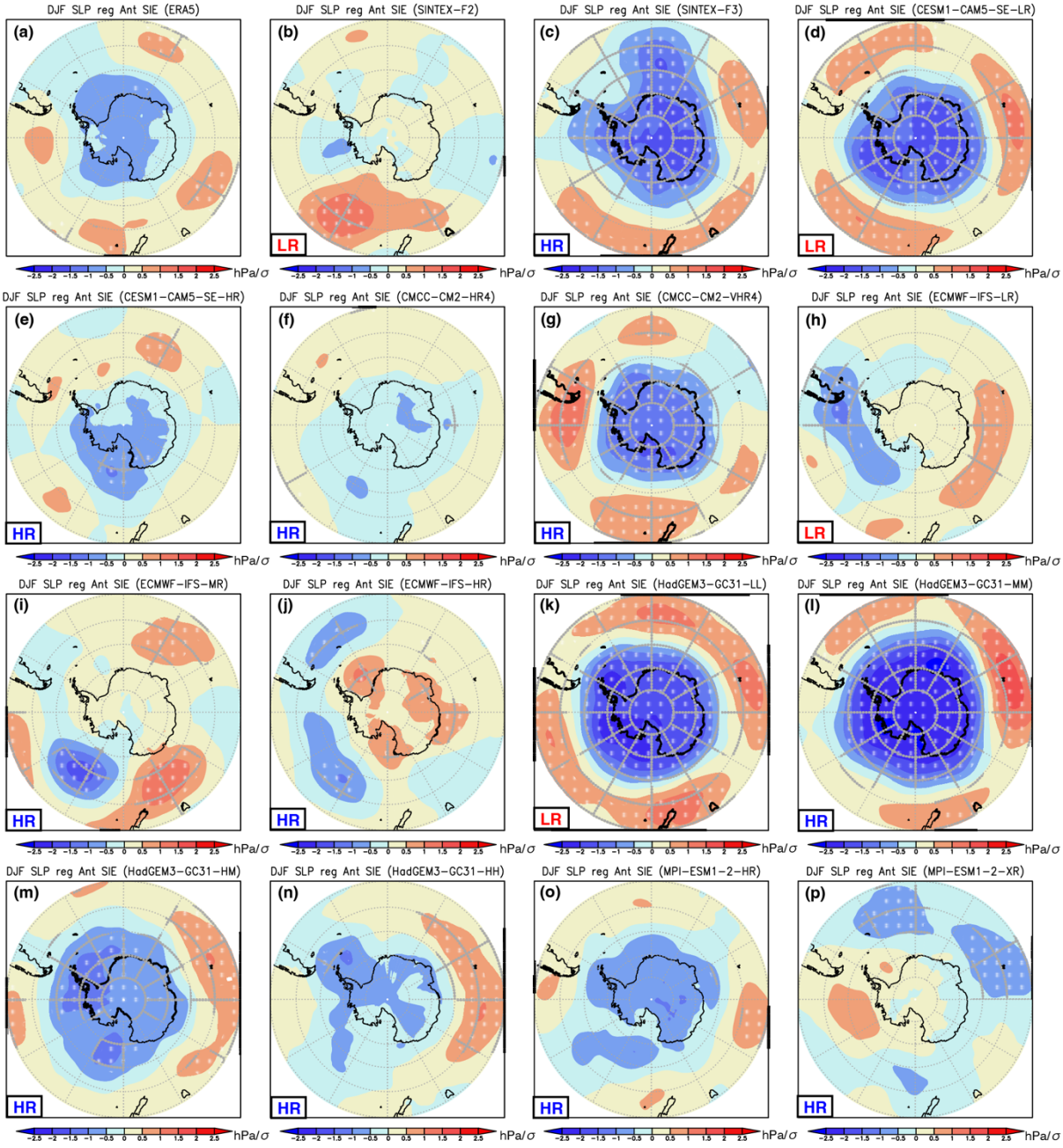

Supplementary Figure 22 (a) Spatial pattern of December-February mean sea level pressure anomalies (SLP; in hPa/ σ) regressed onto the standardized Antarctic sea ice extent (SIE) anomalies for the NSIDC_Nimbus data. A white dot indicate a statistically significant value that exceeds 90 % confidence level using a Student's *t*-test. **(b-p)** Same as in (a), but for the SINTEX-F2, SINTEX-F3, CESM1-CAM5-SE-LR, CESM1-CAM5-SE-HR, CMCC-CM2-HR4, CMCC-CM2-VHR4, ECMWF-IFS-LR, ECMWF-IFS-MR, ECMWF-IFS-HR, HadGEM3-GC31-LL, HadGEM3-GC31-MM, HadGEM3-GC31-HM, HadGEM3-GC31-HH, MPI-ESM1-2-HR, and MPI-ESM1-2-XR models, respectively. The LR in the bottom left of the panel stands for the low-resolution model, whereas the HR corresponds to the high-resolution model.

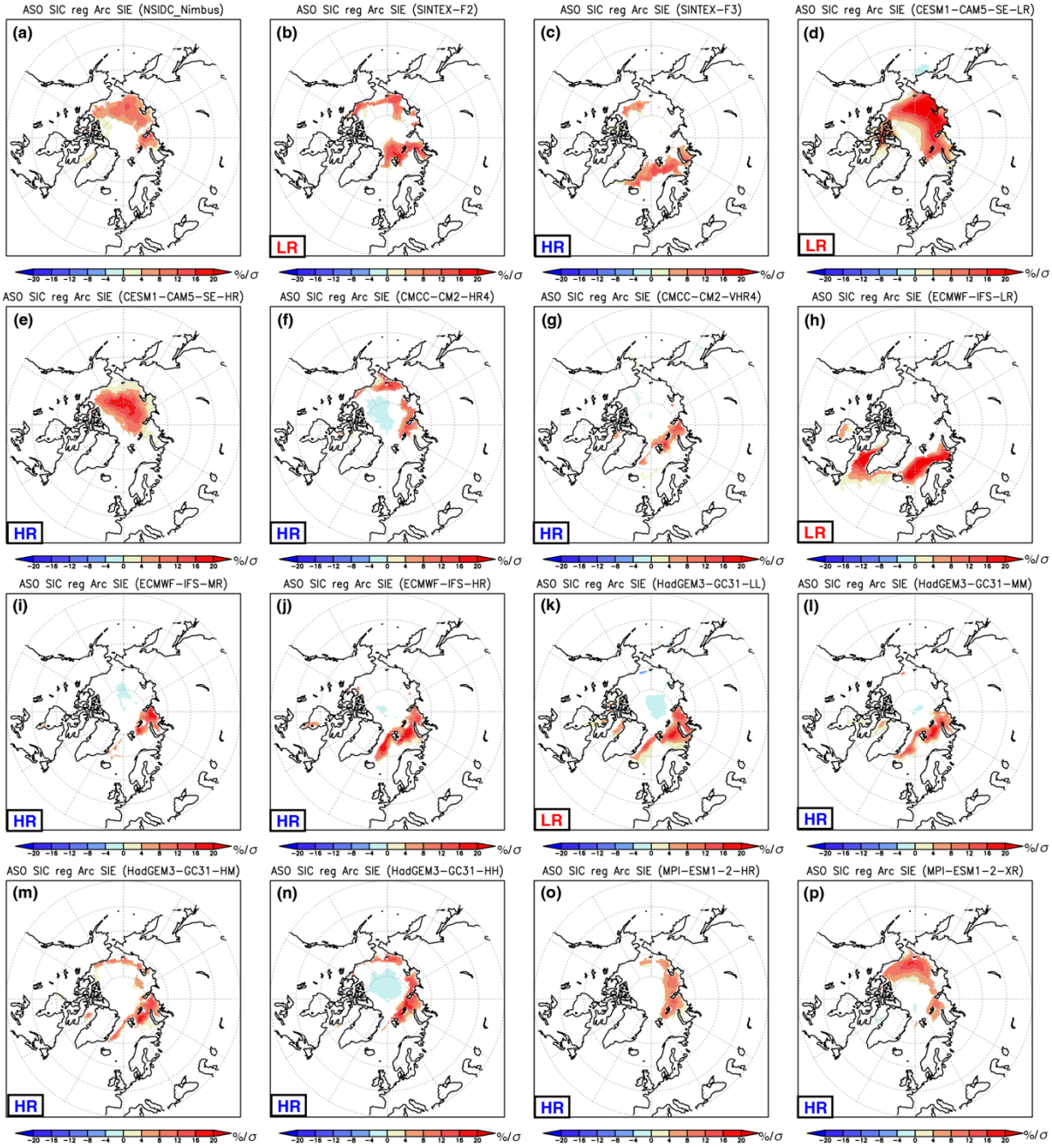

Supplementary Figure 23 (a) Spatial pattern of August-October mean sea ice concentration anomalies (SIC; in %/ σ) regressed onto the standardized Arctic sea ice extent (SIE) anomalies for the NSIDC_Nimbus dataset. Color indicates a statistically significant value that exceeds 90 % confidence level using a Student's *t*-test. **(b-p)** Same as in (a), but for the SINTEX-F2, SINTEX-F3, CESM1-CAM5-SE-LR, CESM1-CAM5-SE-HR, CMCC-CM2-HR4, CMCC-CM2-VHR4, ECMWF-IFS-LR, ECMWF-IFS-MR, ECMWF-IFS-HR, HadGEM3-GC31-LL, HadGEM3-GC31-MM, HadGEM3-GC31-HM, HadGEM3-GC31-HH, MPI-ESM1-2-HR, and MPI-ESM1-2-XR models, respectively. The LR in the bottom left of the panel stands for the low-resolution model, whereas the HR corresponds to the high-resolution model.

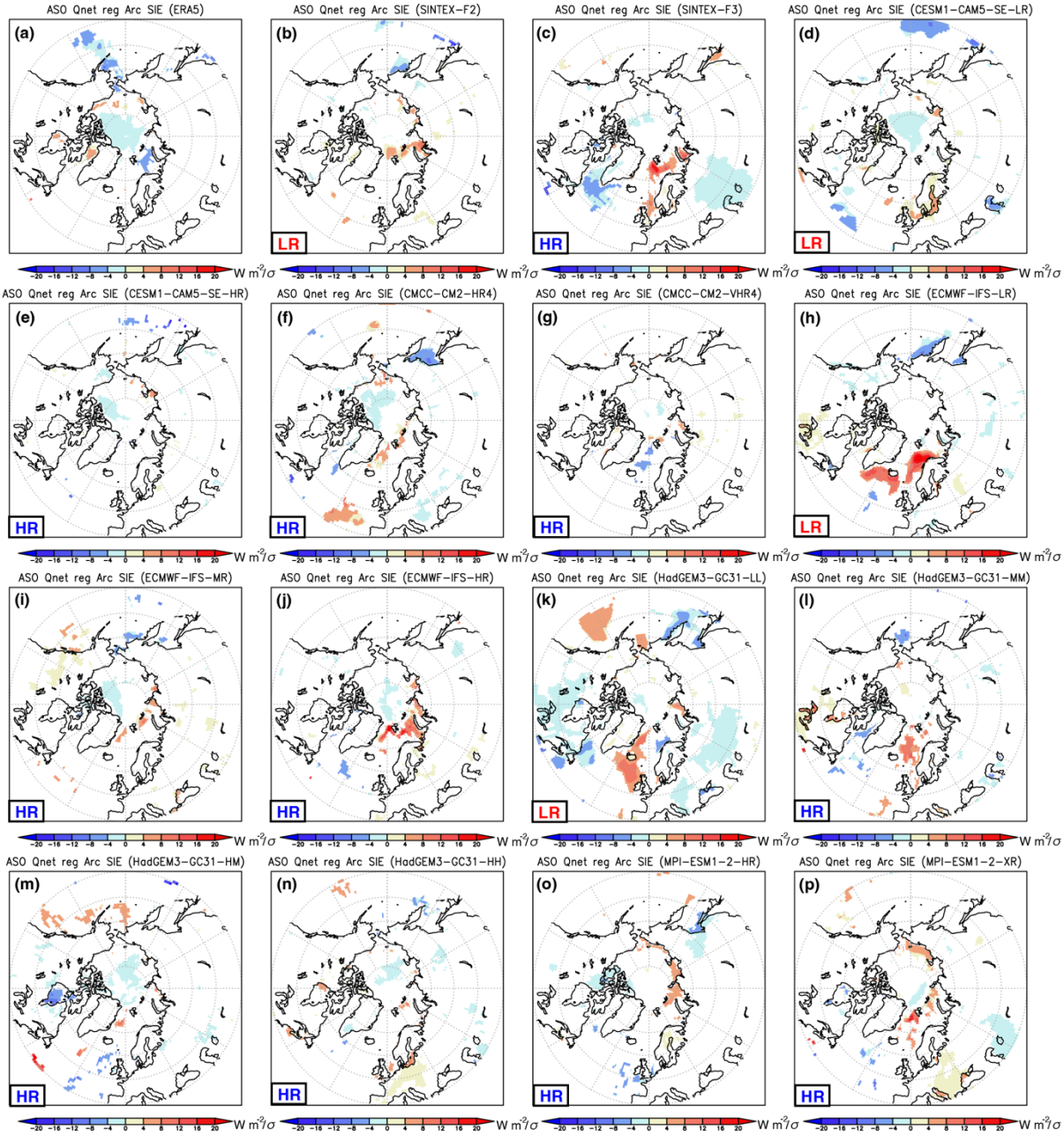

Supplementary Figure 24 (a) Spatial pattern of August-October mean net surface heat flux anomalies (in W m^{-2}/ σ) regressed onto the standardized Arctic sea ice extent (SIE) anomalies for the NSIDC_Nimbus dataset. Color indicates a statistically significant value that exceeds 90 % confidence level using a Student's *t*-test. **(b-p)** Same as in (a), but for the SINTEX-F2, SINTEX-F3, CESM1-CAM5-SE-LR, CESM1-CAM5-SE-HR, CMCC-CM2-HR4, CMCC-CM2-VHR4, ECMWF-IFS-LR, ECMWF-IFS-MR, ECMWF-IFS-HR, HadGEM3-GC31-LL, HadGEM3-GC31-MM, HadGEM3-GC31-HM, HadGEM3-GC31-HH, MPI-ESM1-2-HR, and MPI-ESM1-2-XR models, respectively. The LR in the bottom left of the panel stands for the low-resolution model, whereas the HR corresponds to the high-resolution model.

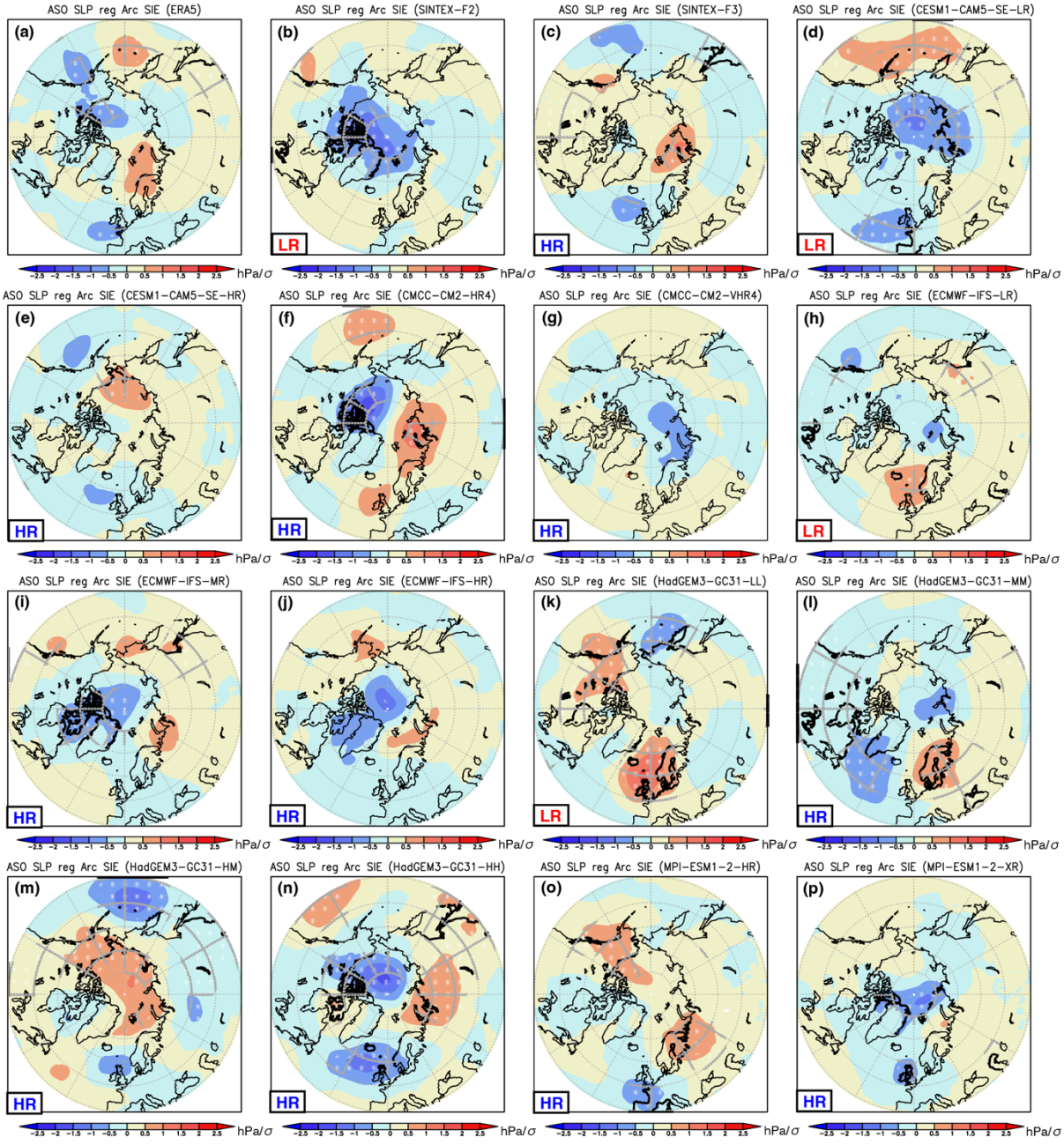

Supplementary Figure 25 (a) Spatial pattern of August-October mean sea level pressure anomalies (SLP; in hPa/ σ) regressed onto the standardized Arctic sea ice extent (SIE) anomalies for the ERA5 reanalysis product. A white dot indicate a statistically significant value that exceeds 90 % confidence level using a Student's *t*-test. **(b-p)** Same as in (a), but for the SINTEX-F2, SINTEX-F3, CESM1-CAM5-SE-LR, CESM1-CAM5-SE-HR, CMCC-CM2-HR4, CMCC-CM2-VHR4, ECMWF-IFS-LR, ECMWF-IFS-MR, ECMWF-IFS-HR, HadGEM3-GC31-LL, HadGEM3-GC31-MM, HadGEM3-GC31-HM, HadGEM3-GC31-HH, MPI-ESM1-2-HR, and MPI-ESM1-2-XR models, respectively. The LR in the bottom left of the panel stands for the low-resolution model, whereas the HR corresponds to the high-resolution model.

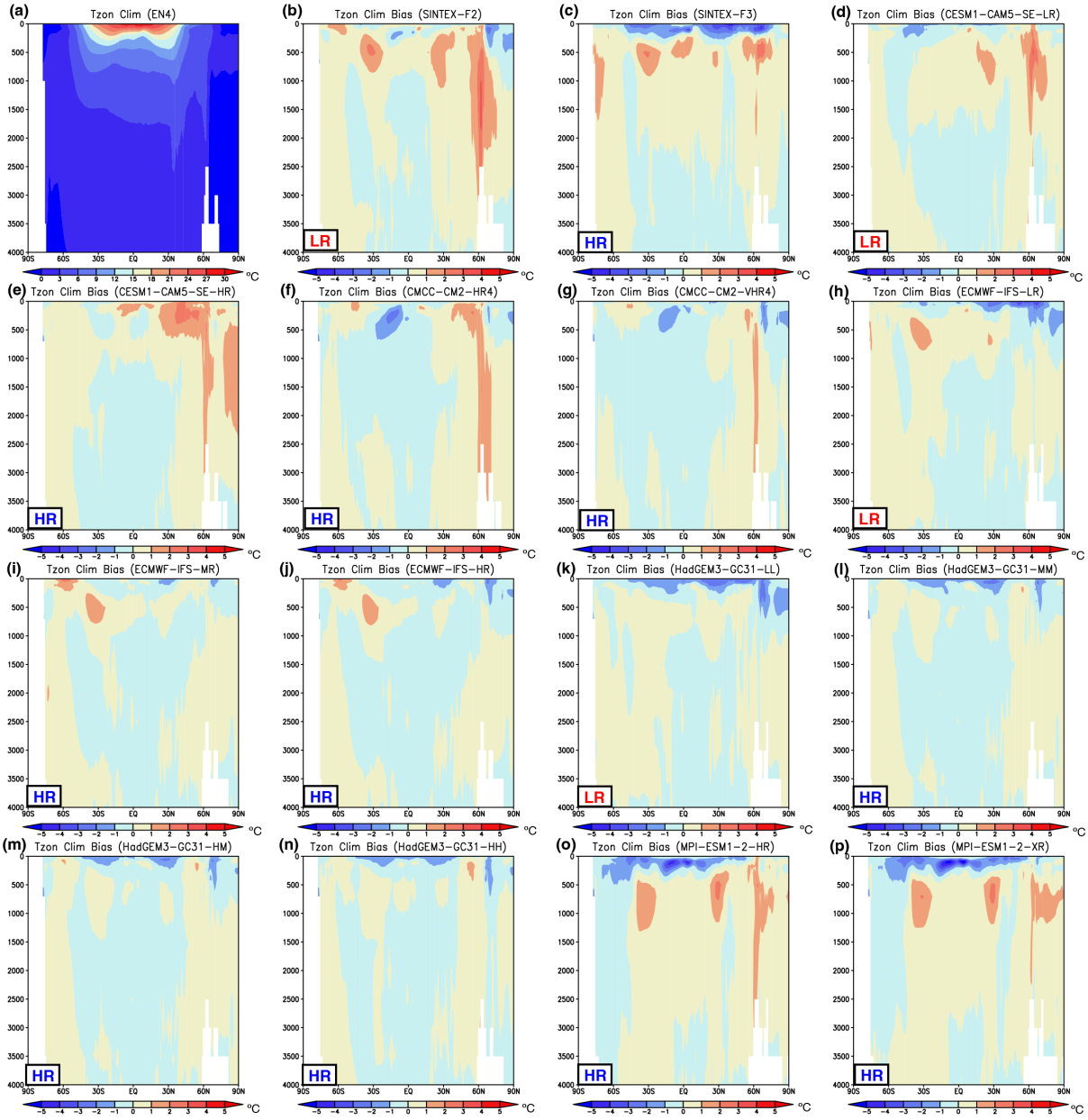

Supplementary Figure 26 (a) Annual mean of zonally-averaged ocean potential temperature (Tzon; in ºC) observed during 1982-2023 as a function of the depth from the EN4 dataset. **(b)** Difference in the annual mean of zonally-averaged ocean potential temperature (in ºC) over the 42 years between the SINTEX-F2 model and EN4 dataset (i.e., model minus observation). **(c-p)** Same as in (b), but for the SINTEX-F3, CESM1-CAM5-SE-LR, CESM1-CAM5-SE-HR, CMCC-CM2-HR4, CMCC-CM2-VHR4, ECMWF-IFS-LR, ECMWF-IFS-MR, ECMWF-IFS-HR, HadGEM3-GC31-LL, HadGEM3-GC31-MM, HadGEM3-GC31-HM, HadGEM3-GC31-HH, MPI-ESM1-2-HR, and MPI-ESM1-2-XR models, respectively. The LR in the bottom left of the panel stands for the low-resolution model, whereas the HR corresponds to the high-resolution model.

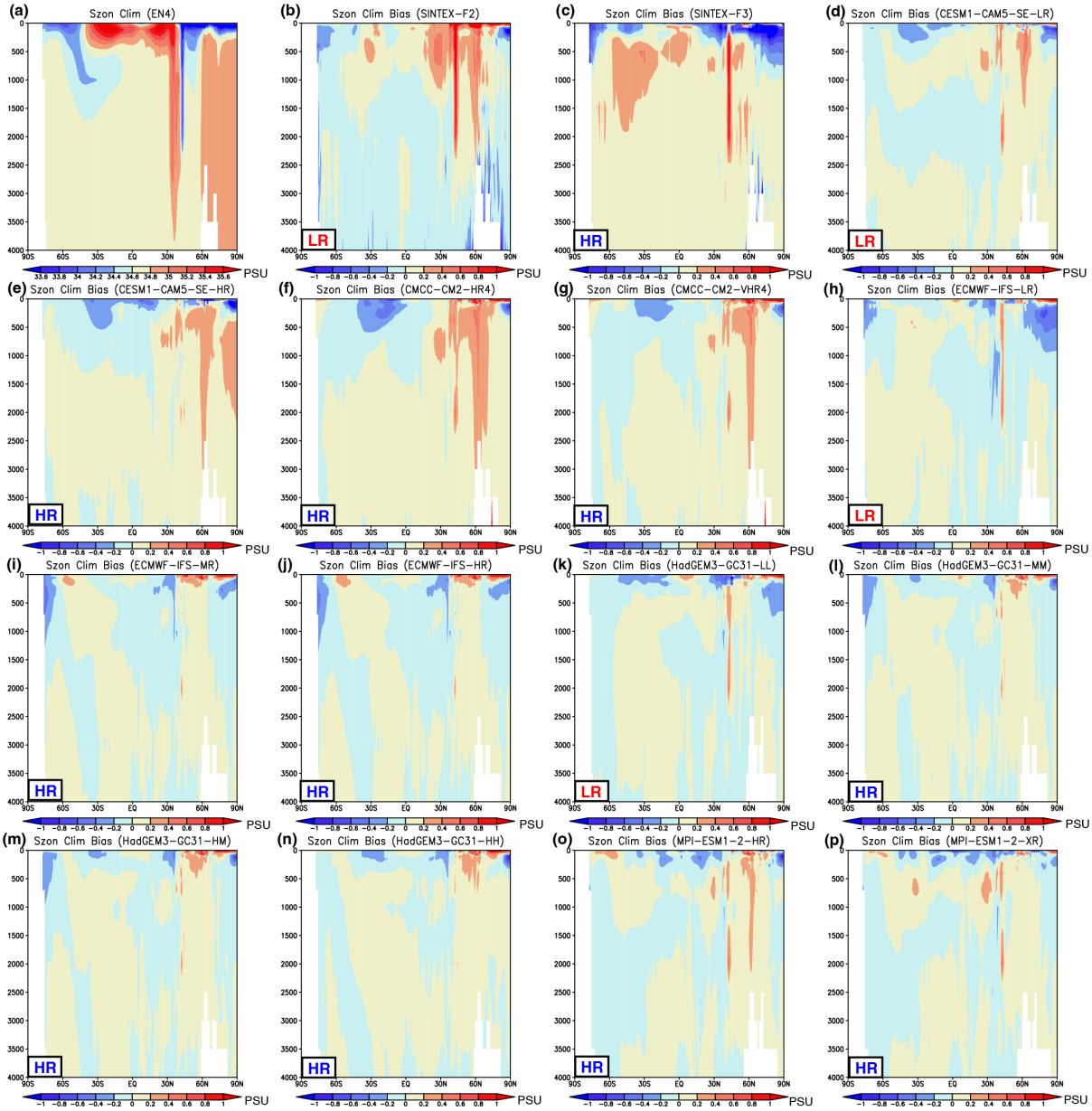

Supplementary Figure 27 (a) Annual mean of zonally-averaged ocean salinity (Szon; in PSU) observed during 1982-2023 as a function of the depth from the EN4 dataset. **(b)** Difference in the annual mean of zonally-averaged ocean salinity (in PSU) over the 42 years between the SINTEX-F2 model and EN4 dataset (i.e., model minus observation). **(c-p)** Same as in (b), but for the SINTEX-F3, CESM1-CAM5-SE-LR, CESM1-CAM5-SE-HR, CMCC-CM2-HR4, CMCC-CM2-VHR4, ECMWF-IFS-LR, ECMWF-IFS-MR, ECMWF-IFS-HR, HadGEM3-GC31-LL, HadGEM3-GC31-MM, HadGEM3-GC31-HM, HadGEM3-GC31-HH, MPI-ESM1-2-HR, and MPI-ESM1-2-XR models, respectively. The LR in the bottom left of the panel stands for the low-resolution model, whereas the HR corresponds to the high-resolution model.

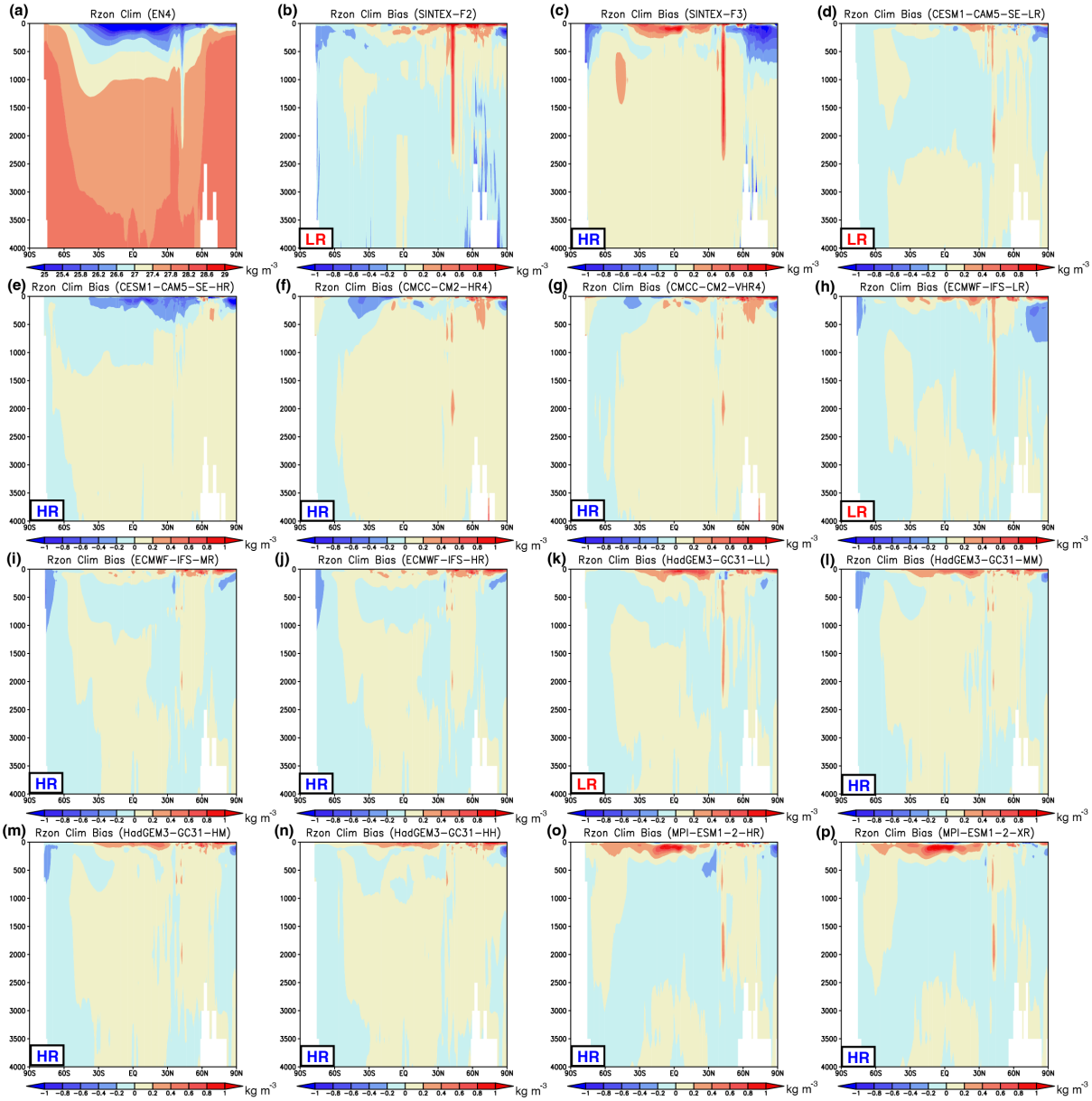

Supplementary Figure 28 (a) Annual mean of zonally-averaged ocean potential density (Rzon; in kg m^{-3}) observed during 1982-2023 as a function of the depth from the EN4 dataset. **(b)** Difference in the annual mean of zonally-averaged ocean potential density (in kg m^{-3}) over the 42 years between the SINTEX-F2 model and EN4 dataset (i.e., model minus observation). **(c-p)** Same as in (b), but for the SINTEX-F3, CESM1-CAM5-SE-LR, CESM1-CAM5-SE-HR, CMCC-CM2-HR4, CMCC-CM2-VHR4, ECMWF-IFS-LR, ECMWF-IFS-MR, ECMWF-IFS-HR, HadGEM3-GC31-LL, HadGEM3-GC31-MM, HadGEM3-GC31-HM, HadGEM3-GC31-HH, MPI-ESM1-2-HR, and MPI-ESM1-2-XR models, respectively. The LR in the bottom left of the panel stands for the low-resolution model, whereas the HR corresponds to the high-resolution model.

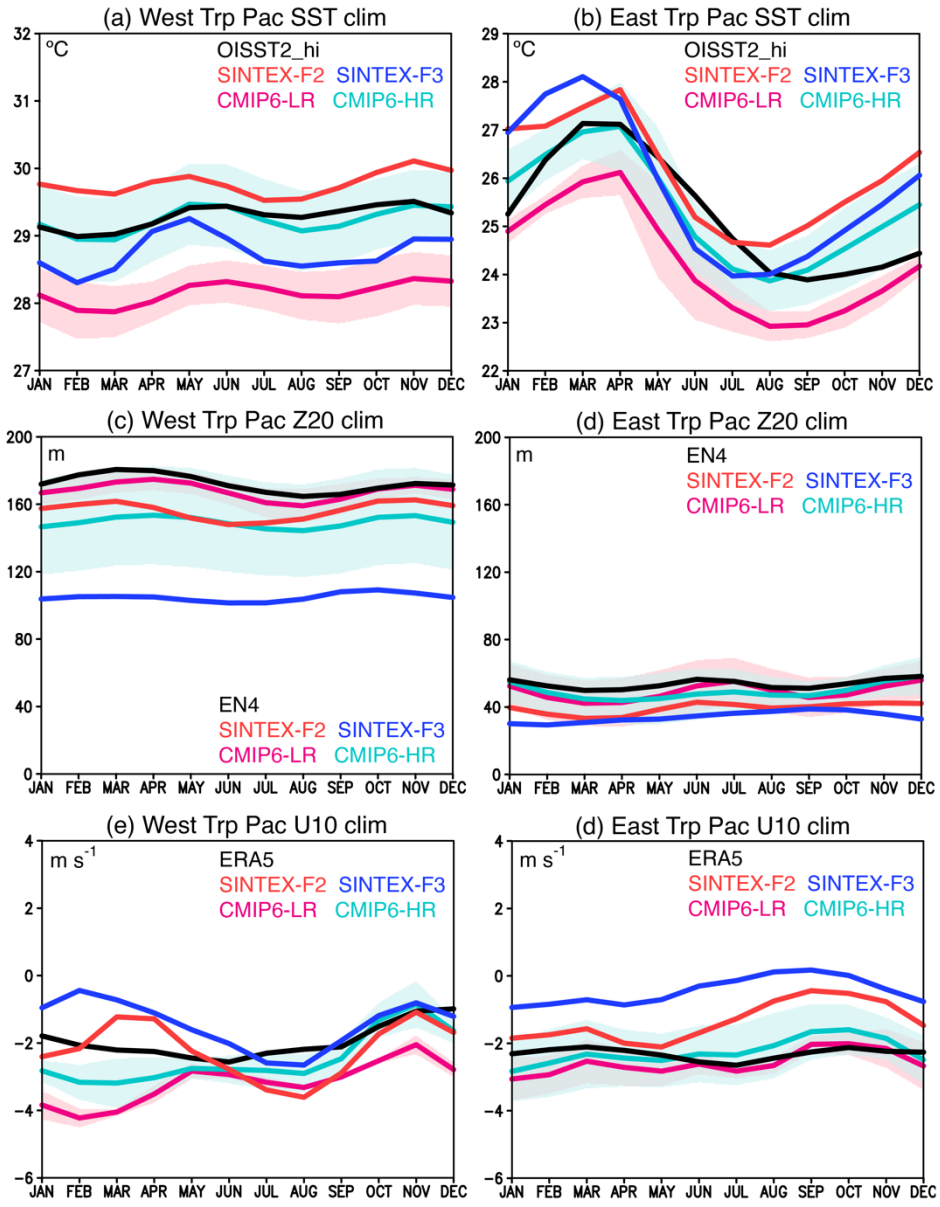

Supplementary Figure 29 (a) Monthly climatology of the western tropical Pacific sea surface temperature (SST; in ºC) for the OISST2_hi (black) dataset, SINTEX-F2 (red), SINTEX-F3 (blue), CMIP6-LR (magenta), and CMIP6-HR (light blue) models. Color shades indicate plus and minus one standard deviation of the model spreads. **(b)** Same as in (a), but for the eastern tropical Pacific SST (in ºC). **(c-d)** Same as in (a-b), but for the thermocline depth (Z20; in m). The observation from EN4 dataset was used. **(e-f)** Same as in (a-b), but for the zonal wind speed at 10 m (U10; in m s^{-1}).